

AD-A073 039

NAVAL OCEAN SYSTEMS CENTER SAN DIEGO CA  
FIBER-OPTIC SONOBUOY LINK DEVELOPMENT - FY 78. FIBER-OPTIC COMP--ETC(U)  
MAR 79 R A EASTLEY, W H PUTMAN

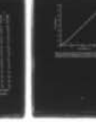
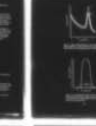
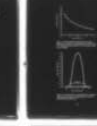
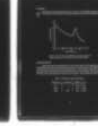
F/G 17/1

UNCLASSIFIED

NOSC/TR-432

NL

1 of 1  
AD  
A073039



END  
DATE  
FILMED  
9-79  
DDC



MICROCOPY RESOLUTION TEST CHART  
NATIONAL BUREAU OF STANDARDS-1963-A

LEVEL 12

# NOSC

NOSC TR 432

NOSC TR-432

DDC  
AUG 23 1979

Technical Report 432

AD A 073039

6

## FIBER-OPTIC SONOBUOY LINK DEVELOPMENT — FY 78

Fiber-optic components for an optical data link to interconnect the submerged hydrophone package with the surface transmitter of a 5-km depth sonobuoy,

16) F11121

12) 46p.

10) R. A. Eastley  
W. H. Putnam

17) WF11121714

11) 27 March 1979

9) Interim Report, 1 October 1977 — 30 September 1978

Prepared for  
Naval Air Development Center

Approved for public release; distribution unlimited.

NAVAL OCEAN SYSTEMS CENTER  
SAN DIEGO, CALIFORNIA 92152

DDC FILE COPY

393 159

LB



NAVAL OCEAN SYSTEMS CENTER, SAN DIEGO, CA 92152

---

**AN ACTIVITY OF THE NAVAL MATERIAL COMMAND**  
**RR GAVAZZI, CAPT, USN**

Commander

**HL BLOOD**

Technical Director

**ADMINISTRATIVE INFORMATION**

The work was sponsored by Code 3043 of the Naval Air Development Center (NADC), Warminster, PA, under the Undersea Target Surveillance block program element 62711N, task area number WF-11-121-710. The work was performed by the authors at Naval Ocean Systems Center (NOSC), EO devices branch, Code 8115 under project number CG22-Fiber Optic Sonobuoy Cable.

Dr. D. J. Albares of NOSC and R. N. Holler of NADC were extremely helpful in providing guidance in fiber optics and sonobuoy system development, respectively. R. J. Gallenberger of NOSC was responsible for the analysis and fabrication of the optical receiver. Dr. S. A. Miller of NOSC was responsible for characterization of the LEDs. Dr. H. E. Rast of NOSC provided data on the Fiber Strength Improvement Program. The development of the 5-km graded index optical fiber was sponsored by the Fiber Optics Technology Program, managed by D. N. Williams of NOSC.

Released by  
M. S. Kvigne, Head  
Communications Research  
and Technology Division

Under Authority of  
H. D. Smith, Head  
Communications Systems  
and Technology Department

REPORT DOCUMENTATION PAGE		READ INSTRUCTIONS BEFORE COMPLETING FORM
1. REPORT NUMBER NOSC Technical Report 432 (TR 432)	2. GOVT ACCESSION NO.	3. RECIPIENT'S CATALOG NUMBER
4. TITLE (and Subtitle) FIBER-OPTIC SONOBUOY LINK DEVELOPMENT - FY 78 Fiber-optic components for an optical data link to interconnect the submerged hydrophone package with the surface transmitter of a 5-km depth sonobuoy	5. TYPE OF REPORT & PERIOD COVERED Interim Report: October 1, 1977 - September 30, 1978	
	6. PERFORMING ORG. REPORT NUMBER	
7. AUTHOR(s) R. A. Eastley W. H. Putnam	8. CONTRACT OR GRANT NUMBER(s)	
9. PERFORMING ORGANIZATION NAME AND ADDRESS Naval Ocean Systems Center San Diego, CA 92152	10. PROGRAM ELEMENT, PROJECT, TASK AREA & WORK UNIT NUMBERS 62711N WF-11-121-710 CG22	
11. CONTROLLING OFFICE NAME AND ADDRESS Naval Air Development Center Warminster, PA	12. REPORT DATE 27 March 1979	
	13. NUMBER OF PAGES 44	
14. MONITORING AGENCY NAME & ADDRESS (if different from Controlling Office)	15. SECURITY CLASS. (of this report) Unclassified	
	15a. DECLASSIFICATION/DOWNGRADING SCHEDULE	
16. DISTRIBUTION STATEMENT (of this Report) Approved for public release; distribution unlimited.		
17. DISTRIBUTION STATEMENT (of the abstract entered in Block 20, if different from Report)		
18. SUPPLEMENTARY NOTES		
19. KEY WORDS (Continue on reverse side if necessary and identify by block number) Fiber Optics                      Data transfer Sonobuoys                        Undersea sensors Undersea cables                Undersea acoustics Electro-optics                  Surface buoys		
20. ABSTRACT (Continue on reverse side if necessary and identify by block number) This report presents the FY78 progress in the development of fiber-optic components for an optical data link to interconnect the submerged hydrophone package with the surface transmitter of a 5-km depth sonobuoy. A Kevlar-49 strengthened, single-fiber sonobuoy cable was tested which met the operational and environmental requirements of a 5-km depth, 50 kb/s data rate, duplex sonobuoy. Optical fibers were fabricated which satisfy length and optical requirements. Tests of a link consisting of an LED, a 5-km fiber, and an optical receiver showed that, when the estimated losses for the other link components such as duplexers, connectors and splices are included, there is <span style="float: right;">7m</span>		

UNCLASSIFIED

SECURITY CLASSIFICATION OF THIS PAGE (When Data Entered)

sufficient optical power available (18dB margin) with present technology to meet deep sonobuoy link transmission requirements.

UNCLASSIFIED

SECURITY CLASSIFICATION OF THIS PAGE (When Data Entered)

## OBJECTIVE

Develop the fiber-optic components for an optical data link to interconnect the submerged hydrophone package with the surface transmitter of a 5-km depth sonobuoy.

## RESULTS

1. A Kevlar-49 strengthened fiber optic cable was tested which met the mechanical and environmental requirements of a 5-km depth sonobuoy.
2. Optical fibers were fabricated which satisfy length and optical requirements.
3. Tests of a link consisting of an LED, a 5-km fiber, and an optical receiver showed that, when the estimated losses for the other link components such as duplexers, connectors and splices are included, there is sufficient optical power available (18-dB margin) with present technology to meet deep sonobuoy link transmission requirements.

## RECOMMENDATIONS

1. Test the fiber-optic cable under load in a water environment.
2. Continue to improve fiber strength and durability to make the strain characteristics compatible with the Kevlar strength members.
3. Evaluate duplex couplers for deep sonobuoy applications.
4. Support development of 1.0 to 1.3  $\mu\text{m}$  light emitting diodes (LEDs) and detectors to utilize the lower fiber attenuation at long wavelengths.
5. Standardize LED coupled power specifications.
6. Establish a technique for reliably splicing optical fiber pigtails to the optical components of the link.
7. Develop cable winding, payout, braking, and wave-motion isolation techniques.
8. Investigate the pressure tolerance of LEDs, photodiodes, and duplexers.
9. Develop optical pressure-housing feedthroughs and connectors.

Accession For	
NTIS GRA&I	<input checked="" type="checkbox"/>
DDC TAB	<input type="checkbox"/>
Unannounced	<input type="checkbox"/>
Justification	
By _____	
Distribution/	
Availability Codes	
Dist	Avail and/or special
A	

## CONTENTS

INTRODUCTION . . . page 5

KEVLAR STRENGTHENED CABLE . . . 6

- Cable Development . . . 6
- Cable Tests . . . 6
- Attenuation Coiled/Uncoiled . . . 8
- Attenuation Under Load . . . 9
- Attenuation Versus Temperature . . . 9
- Attenuation Versus Pressure . . . 9
- Breaking Strength . . . 12
- Loaded Flexure . . . 12
- Torque Balance . . . 13
- Cable Roundness . . . 13

FIBER DEVELOPMENT . . . 13

- High Strength 5-km Step-Index Fiber Development . . . 13
- High Strength 5-km Graded-Index Fiber Development . . . 16
- Triple-Core Fiber for Duplex Communication . . . 19
- Cabled Fiber Strength Requirement . . . 19
- Fiber Strength Improvement Program . . . 21

5-km LINK DEMONSTRATION . . . 23

- Introduction . . . 23
- Optical Power Performance . . . 24
- Link Performance Estimate . . . 27

CONCLUSIONS . . . 28

RECOMMENDATIONS . . . 30

REFERENCES . . . 31

APPENDIX A: LED COUPLED POWER CALCULATION . . . 33

APPENDIX B: FIBER RESPONSE FACTOR,  $\eta_f$

APPENDIX C: SIDE-LIGHT CORRECTION FACTOR,  $\eta_s$ , FOR EDGE-EMITTER LEDS . . . 39

APPENDIX D: RECEIVER SENSITIVITY . . . 43

## ILLUSTRATIONS

- 1 Fiber optic sonobuoy cable design . . . page 6
- 2 Fiber optic sonobuoy cable attenuation on two spool sizes . . . 8
- 3 Cabled fiber attenuation under load . . . 9
- 4 Cabled fiber attenuation vs temperature . . . 10
- 5 Cabled fiber attenuation vs pressure . . . 11
- 6 NA scan pattern for cabled fiber . . . 12
- 7 Five-km step-index optical fiber . . . 14
- 8 Five-km step-index optical fiber attenuation . . . 15
- 9 NA scan pattern for 5-km step index fiber . . . 16
- 10 Five-km graded-index optical fiber . . . 17
- 11 Five-km graded-index optical fiber attenuation . . . 18
- 12 NA scan pattern for 5-km graded-index optical fiber . . . 18
- 13 Cross-section of triple-core optical fiber . . . 19
- 14 Triple-core fiber attenuations . . . 20
- 15 NA scan pattern for triple-core fiber (core 1) . . . 20
- 16 Sonobuoy duplex link schematic . . . 23
- 17 Measured coupled powers for 0.8 to 0.9  $\mu\text{m}$  LEDs as a function of drive current . . . 26
- 18 NOSC receiver sensitivity . . . 27
- 19 Five-km wideband link demonstration . . . 28
- A-1 Total power vs drive current for typical edge emitter LED . . . 35
- A-2 Far-field pattern (angular distribution of typical edge-emitter LED . . . 36
- A-3 Emitting area of typical edge-emitter LED . . . 37
- C-1 Light emitted from the sides of the LED is not coupled into the fiber . . . 39
- C-2 Geometry for computing relative intensities of light emitted from face ( $A_f$ ) and sides ( $A_s$ ) of edge-emitter LEDs . . . 41
- C-3 Side-light correction factor,  $\eta_s$  . . . 42

## TABLES

- 1 Kevlar cable objectives . . . page 7
- 2 ITT manufacturing data for the Kevlar cable . . . 7
- 3 Cabled fiber NA . . . 11
- 4 Cable breaking strength . . . 13
- 5 ITT manufacturing data for 5-km step index fiber . . . 14
- 6 Step index numerical apertures . . . 15
- 7 ITT manufacturing data for 5-km graded index fiber . . . 17
- 8 Graded index fiber numerical aperture . . . 17
- 9 Triple-core fiber numerical aperture . . . 21
- 10 LED coupled power,  $P_c$ , into a fiber . . . 25
- A-1 LED coupled power into a fiber . . . 34

## INTRODUCTION

This report presents the FY 78 progress in the development of fiber-optic components for an optical data link to interconnect the submerged hydrophone package with the surface transmitter of a 5-km depth sonobuoy. The sonobuoy optical link consists of an optical transmitter containing a light emitting diode (LED) and an LED driver, duplexers for two-way transmission, the interconnecting optical fiber cable, an optical receiver (detector and amplifier), pressure housing feedthroughs, and connectors. Optical fibers can be used in sonobuoys to provide high bandwidth (several Mb/s for step-index fibers and hundreds of Mb/s for graded-index fibers) and to eliminate problems encountered when using single-conductor, sea-return electrical wires in cables interconnecting deep hydrophones with the surface transmitter. Problems that will be eliminated are

- (a) complex filtering required to compensate for the inductance of the amount of wire left in the coil,
- (b) signal loss caused by pinholes in the cable insulation, and
- (c) the high electrical wire impedance at the required bandwidth of deep sonobuoy applications.

A pacing item in this development has been the achievement of 5-km fibers having the strength to withstand cabling and operational stresses. In the analysis presented in the Cabled Fiber Strength Requirement section of this report it is concluded that, in order for the fiber to survive a momentary deployment strain of 1.2% and a 3-hour operating strain of 0.9%, the fiber must pass a 1.4% strain proof test. Very strong (1% proof test strain (elongation)), low loss (less than 5 dB/km) fibers are being produced routinely and proof test strains of 1.5% in lengths greater than 5 km have been reported to have been achieved in the laboratory.\* It is the goal of the Fiber Strength Improvement Program, funded by Defense Advanced Research Projects Agency (DARPA) through 1978 and by Naval Material Command (NAVMAT) in 1979 and beyond, to develop 10-km fibers that can routinely withstand 2-3% proof test strains. A discussion of progress in the Fiber Strength Improvement Program is included here for completeness.

Another pacing item has been the development of a fiber-optic cable exhibiting minimal attenuation increase when the fiber is cabled and when the cable is subjected to sonobuoy operational, environmental, and mechanical stresses such as 48 MPa (7 kpsi) pressure, -50° to +70°C temperature, 1.9-cm bend radius, and 330 N (75 lb) cable load. The approach has been to incorporate optical fibers and strength members into cables and to test the cables to sonobuoy specifications.

Development of the optical data link required evaluation of candidate transmitter and receiver components on a cost/performance basis, design and fabrication of a 50 kb/s receiver, and fabrication and tests of a 5-km laboratory link for power margin and bit error rate.

In FY 77-78 major milestones were achieved in the fiber-optic sonobuoy link project with the development of a Kevlar-49 strengthened sonobuoy cable, a 5-km step-and-graded-index fiber, and a high sensitivity 50-kb/s optical receiver. Test results of the cable, a 5-km fiber, a triple-core fiber/cable, and a fiber-optic data link are presented in this report.

\*Adolph Asam, ITT/Electro-Optical Products Division, private communication, unpublished data.

Progress in the project through FY 76 and FY 77 is detailed in references 1 and 2. Included for completeness is a discussion of the a 5-km graded-index fiber development funded by NAVMAT.

## KEVLAR STRENGTHENED CABLE

### CABLE DEVELOPMENT

The Kevlar cable was designed and fabricated at ITT, Roanoke, VA under contract N00123-77-C-0079. The 1-km cable contains a centrally-located optical fiber, two contra-helically laid layers of Kevlar strength members, and an outer nylon braid, figure 1.<sup>2</sup> The cable design is "open," which allows the water to flood the cable, alleviating hydrostatically-induced microbend losses. Manufacturing objectives for the Kevlar cable are listed in table 1.<sup>3</sup> ITT data for the manufactured cable is listed in table 2.

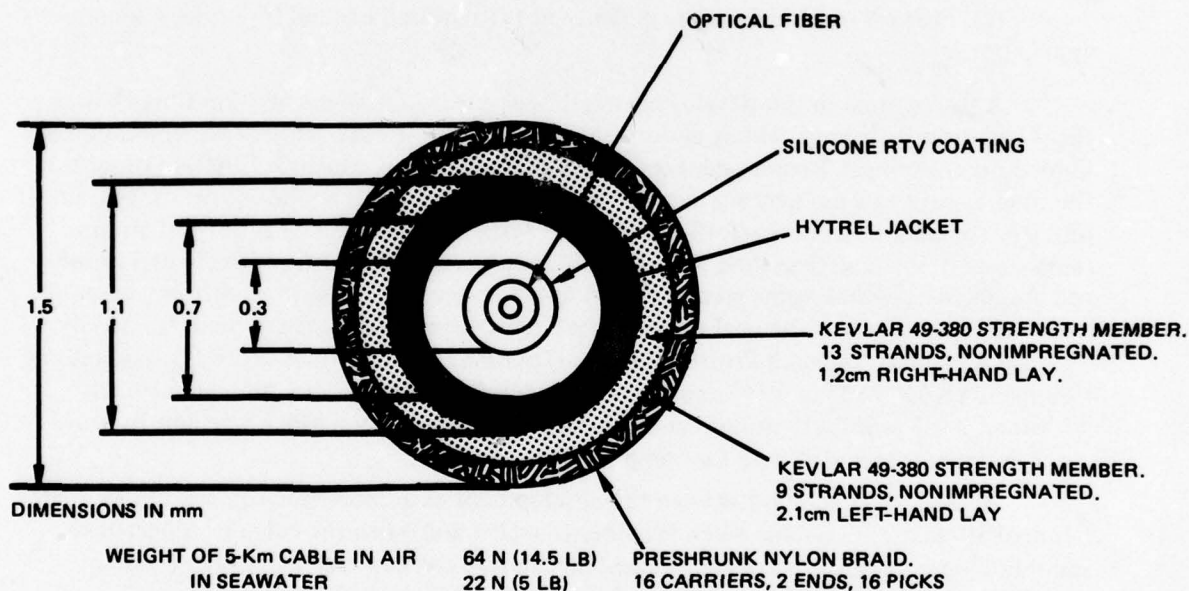


Figure 1. Fiber-optic sonobuoy cable design.

### CABLE TESTS

Optical attenuation and numerical aperture tests were conducted by NOSC. Mechanical tests were conducted under contract 66001-78-M-5141 at Nevada Engineering and Technology Corp (NETCO), Long Beach, CA. Cabled fiber tests conducted by NOSC were

1. NOSC TR 148, "Fiber Optic Sonobuoy Cable Development FY76," by R. A. Eastley, 8 August 1977.
2. NOSC TR 297, "Fiber Optic Sonobuoy Cable Development FY77," by R. A. Eastley and W. H. Putnam, 15 August 1978.
3. Final Report, Contract N00123-77-C-0079, "Follow-on Development of Fiber Optic Cables for Sonobuoy Systems," 5 April 1978, ITT/EOPD.

Table 1. Kevlar cable objectives.

Length, km	1 10 capability
Diameter, mm	1.47
Strength, at 2% strain, N(lb)	1245(280)
Attenuation, dB/km @ 0.82 $\mu\text{m}$	4.5 8.0 required
Excess cabling loss, dB/km	1
Torque balance	balanced at 330 N, in air
Coiled configuration	canister, 3.8-4.5 cm tapered I.D.
Pressure, MPa(kpsi)	to 70(10)

Table 2. ITT manufacturing data for the Kevlar cable.

Length, km	1.001
Diameter, mm	1.5
Strength at 2% strain, N (lb)	1245(280)
Weight in air N(lb)	17.6(3.95)
Fiber type	Step index
designation number	SCVD-10343 Batch 072977-DEK-2.
core, $\mu\text{m}$	43
clad, $\mu\text{m}$	125
coating, $\mu\text{m}$	300
buffer, $\mu\text{m}$	700
Fiber dispersion @ 3 dB, ns/km before cabling, on spool	8.42
after cabling, strung,	8.11
coiled configuration	8.19
Fiber attenuation, at 0.82 $\mu\text{m}$ , dB/km	
before cabling, strung	5.75
after cabling, strung	5.97
24 hrs after cabling, strung	6.03
Coiled configuration	7.13
Numerical aperture, before cabling	0.31
after cabling (0.01 precision)	0.30
Torque balance at 330 N load, Nm (newton-meters)	$6.9 \times 10^{-3}$
Pressure resistance	open design

- (a) attenuation (coiled and uncoiled),
- (b) attenuation under load,
- (c) attenuation as a function of temperature,
- (d) attenuation as a function of pressure,
- (e) fiber numerical aperture.

Cable tests conducted at NETCO were

- (a) breaking strength,
- (b) loaded flexure,
- (c) torque balance.

#### ATTENUATION COILED/UNCOILED

Optical attenuation for the unloaded cable in a 3.8-cm diameter coil (simulating sonobuoy cable pack wind), and a 16-cm diameter coil (simulating strung) are shown in figure 2. The optical attenuation increase in the cable pack configuration is typically 1.5 dB/km. The wavelengths under consideration for the sonobuoy are 0.8 to 0.9  $\mu\text{m}$  and greater than 1  $\mu\text{m}$ .

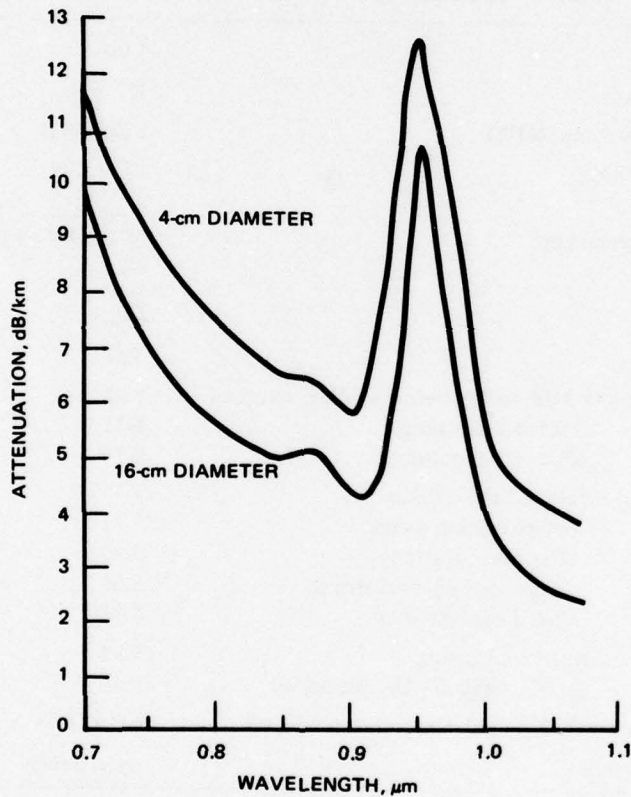


Figure 2. Fiber optic sonobuoy cable attenuation on two spool sizes. Cable optical attenuation as a function of wavelength is shown for the unloaded cable wound on a 4-cm diameter spool and a 16-cm diameter spool. The launch numerical aperture was 0.1 and precision was  $\pm 0.4$  dB/km.

### ATTENUATION UNDER LOAD

For this measurement, a 320-m length of the cable was strung between six 30-cm-diameter freely-rotating pulleys. The pulley separation was 80 meters. Weights were applied to one end in 44-N (10-lb) increments from 22 N (5 lb) up to 422 N (95 lb). No change in attenuation was observed when the cable was subjected to the test loads. This achievement is a major improvement over the first ITT cable, which used steel as the strength member. Test results for both cables are shown for comparison in figure 3.

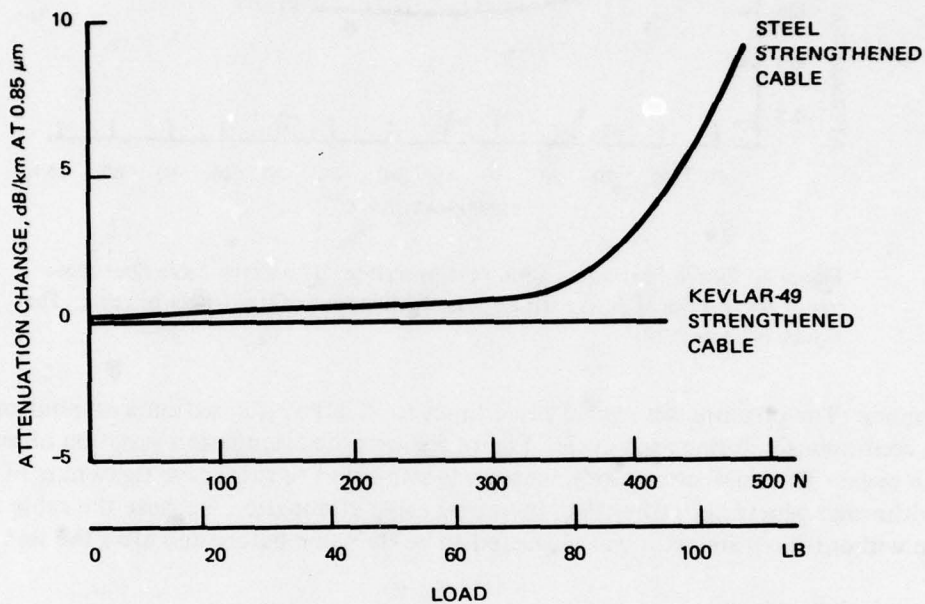


Figure 3. Cabled fiber attenuation under load. Attenuation as a function of load is shown for both the Kevlar-49 cable and the earlier steel-strengthened cable. The operational load is 330 N. In the steel-strengthened cable, the fiber broke at 480 N. The launch NA was 0.24 and the length was 325 m.

### ATTENUATION VERSUS TEMPERATURE

A 400-m length of the cable was subjected to temperatures from  $-50^{\circ}$  to  $+70^{\circ}\text{C}$ . The temperature was stabilized at  $+20^{\circ}$ ,  $-50^{\circ}$ , and  $+70^{\circ}\text{C}$ ; fiber attenuation was measured continuously over the range of variation. Figure 4 shows the optical attenuation as a function of temperature change. The maximum attenuation change noted was 0.3 dB/km. After one hour of stabilization at  $+20^{\circ}\text{C}$  at the end of the test, the fiber attenuation returned to the same value of attenuation measured at the start of the temperature test.

### ATTENUATION VERSUS PRESSURE

A 400-m length of the cable was subjected to hydrostatic pressure from 0 to 70 MPa (10 kpsi) to determine the optical attenuation variation as a function of pressure. A feed-through penetrator was fabricated to bring the optical fiber into and out of the pressure

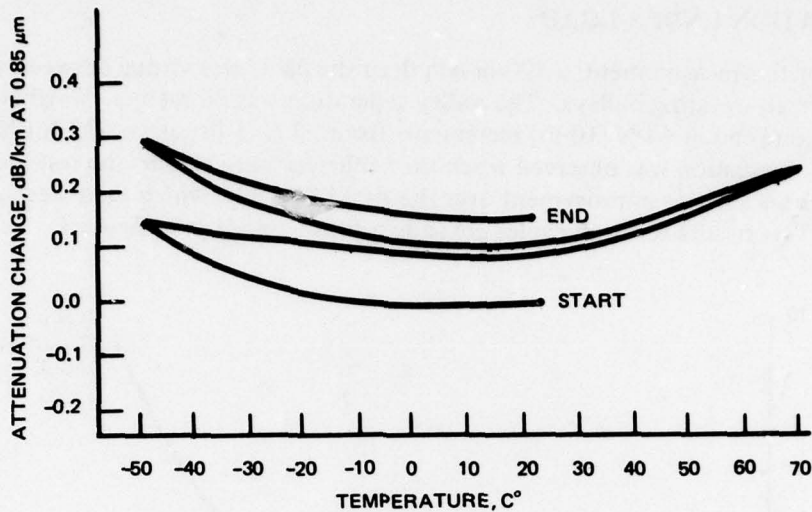


Figure 4. Cabled fiber attenuation vs temperature. The Kevlar cable fiber attenuation was measured during temperature cycling for a 400-m length of cable. The launch NA was 0.24.

chamber. The pressure was cycled three times to 70 MPa; attenuation was monitored at 0.85  $\mu\text{m}$  continuously during each cycle. Figure 5 shows the attenuation variation observed for each cycle. The small attenuation increase is attributed to successive tightening of the feedthrough penetrator rather than increased cable attenuation, because the cable attenuation without the penetrator was measured to be the same before and after the test.

#### Numerical Aperture

Light incident on a fiber that is at an off-axis angle  $\theta$  will be accepted by the fiber if:<sup>4</sup>

$$\sin \theta < \text{NA} \quad (1)$$

where

$$\text{NA} = \text{numerical aperture } (n_1^2 - n_2^2)^{1/2}$$

$n_1$  = refractive index of core

$n_2$  = refractive index of clad

A method of measuring the fiber NA, which is used by NOSC, is to illuminate the input end with a large NA lens and scan the fiber output in the far field with a small detector.<sup>5</sup> The angle,  $2\theta_m$ , is measured between 10% intensity points on the scan pattern. Measurements were performed with a 0.85- $\mu\text{m}$  source for lengths up to 500 m and with an unfiltered white light source for longer lengths. The launch NA was 0.5 and the detector resolution was 0.6°

4. DoD STD 1678 Fiber Optical Test Methods and Instrumentation.

5. NOSC contract N66001-77-C-0137, "Development and Fabrication of High Strength Long Length Optical Fiber," ITT/EOPD.

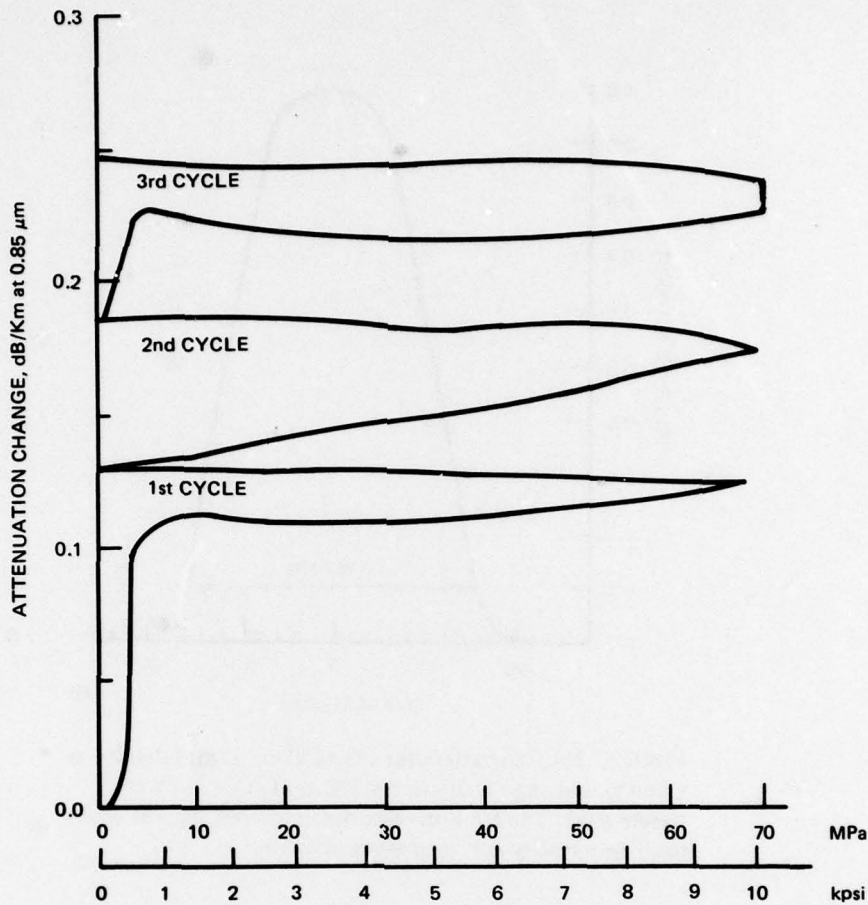


Figure 5. Cabled fiber attenuation vs pressure. The attenuation change is attributed to feedthrough penetrator tightening on the fiber, rather than increased cable attenuation, because the cable attenuation without the penetrator was measured to be the same before and after the test. The launch NA was 0.24 and the length was 400 m.

(0.01 NA). ITT measured the fiber NA by imaging a white light source onto the fiber end using a 0.5-NA lens and visually observing the far-field pattern on a screen having calibrated rings for determining NA.

Results of both measurement methods are shown in table 3. Figure 6 shows a far field pattern obtained using the scan method.

Table 3. Cabled fiber NA.

Measured by	Length (m)	Method	NA
ITT	1	Visual	0.31
NOSC	1	Scan	0.301
NOSC	500 on 3.8-cm spool	Scan	0.251
NOSC	400 on 16-cm spool	Scan	0.256

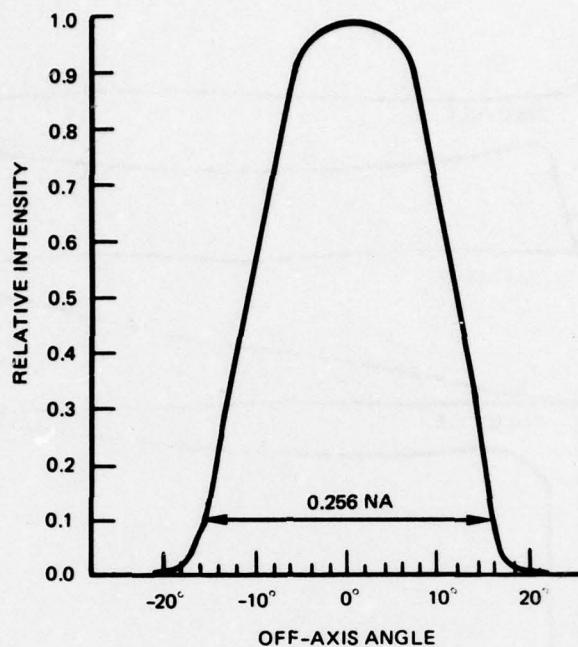


Figure 6. NA scan pattern for cabled fiber. Light intensity as a function of angle is shown for 500 m of cable ( $0.85 \mu\text{m}$  wavelength). The NA is the sine of the off-axis angle at which the light intensity is 10% of the peak value.

There is close agreement in NAs measured by ITT (visual) and NOSC (scan) over 1-m lengths. There is little difference in the NAs measured with the cable in a tight wind (3.8-cm diameter, 500-m length) or a loose wind (16-cm diameter, 400-m length).

### BREAKING STRENGTH

The strength of the Kevlar strength members was tested at NETCO. Four cable samples of 2.5-m gage lengths were tested on an Instron Universal Testing Machine. Each cable sample was gripped on 15-cm-diameter drums at each end to minimize bending stress. The grooved drums were lined with double-stick masking tape to minimize cable slippage. Cable strain was monitored by Instron crosshead movement. The results of the tests are listed in table 4.

These results imply that when the cable is loaded to the operational load for several hours, a strain of at least 0.9% is imposed on the fiber.

### LOADED FLEXURE

At NETCO, loaded flexure tests were conducted by stretching cable samples between two 10-cm-diameter sheaves at various loads. The cables were flexed by rotating the sheaves  $\pm 28^\circ$ . Three samples were loaded to 310 N(70 lb), 470 N(105 lb), and 620 N(140 lb), respectively. Optical continuity of the fiber was monitored after every 5000 cycles. No cable wear or loss of optical continuity were observed at any load up to 100,000 cycles, when the tests were terminated.

Table 4. Cable breaking strength.

Sample	Breaking Load, N(lb)	Strain <sup>a</sup> %, at 330 N(75 lb)
1	1323 (297.5)	0.88
2	b	0.78
3	1352 (304)	0.79
4	1361 (306)	0.78

- a. Strain (elongation) measured after 5 cycles to 890 N(200 lb). When cable was loaded to 330 N(75 lb), it strained an additional 0.1%, typically in 5 minutes.
- b. The cable slipped on the drum at 1169 N(263 lb), kinked, and broke at 1105 N(248 lb).

### TORQUE BALANCE

The torque was measured by NETCO by loading three 3-m lengths of cable with a 330 N(75 lb) dead weight. The force required to prevent a collar, clamped to the cable, from rotating was used to compute the torque. NETCO measured torques of  $0.6 \times 10^{-3}$ ,  $3.2 \times 10^{-3}$ , and  $4.4 \times 10^{-3}$  newton meters (Nm). ITT conducted a similar test prior to delivery of the cable.<sup>3</sup> The torque was measured to be  $6.1 \times 10^{-3}$  and  $7.8 \times 10^{-3}$  Nm on two samples. These torques are negligible compared to other rotational forces on the sonobuoy submerged unit.

### CABLE ROUNDNESS

One of the problems identified in the previous twisted-steel cable design was the lack of cable roundness (reference 1). This problem was addressed in the present Kevlar cable design by the use of coaxial armor layers. The cable diameter, measured in two orthogonal axes at 100-meter intervals, was between 1.49 and 1.54 mm (1.47 mm maximum specified).

### FIBER DEVELOPMENT

#### HIGH STRENGTH 5-km STEP-INDEX FIBER DEVELOPMENT

A 5-km step-index optical fiber was developed under NOSC contract N66001-77-C-0137 at ITT Electro-Optical Products Division, Roanoke, VA.<sup>5</sup> The goals were to fabricate a 5-km fiber having less than 7 dB/km attenuation at  $0.85 \mu\text{m}$ , 0.23 NA (min.),  $40 \mu\text{m}$  (min.) core diameter and high strength (proof test to 1% strain without breakage). All contract goals were exceeded, as detailed in the following paragraphs.

ITT's standard preform dimensions limited the length to less than 3 km. To increase the length to the required 5 km, ITT started with 25-mm-diameter substrate tubes (rather than 15 mm); the length of the tube was the standard 54 cm, allowing it to be drawn using available equipment without major modification. In order to maintain reasonable deposition times with the larger preform substrates the deposition speed was increased by a factor of 2 by adding helium to the oxygen gas and by doping the core with phosphorous oxide. Preform roundness was improved by collapsing the substrate under pressure.

Fibers drawn from the first large-diameter preforms were extremely weak. Poor fiber strength was attributed to the lower quality of the commercial grade TO-8 silica substrate tubes available in the 25-mm diameter compared to 15 mm. After investigating improved quality substrate materials such as TO8-FB, TO8-WG, and Suprasil 2, ITT concluded that TO8-FB grade silica substrates are necessary for production of high strength optical fibers. In addition, the substrate was laser polished before deposition and after collapse to heal the cracks, and the fiber was drawn and coated in a clean environment.

The delivered fiber, figure 7, which was the longest known high-strength fiber produced to date, was proof tested to 1% elongation over its entire 5-km length. Manufacturing data for the fiber is shown in table 5.

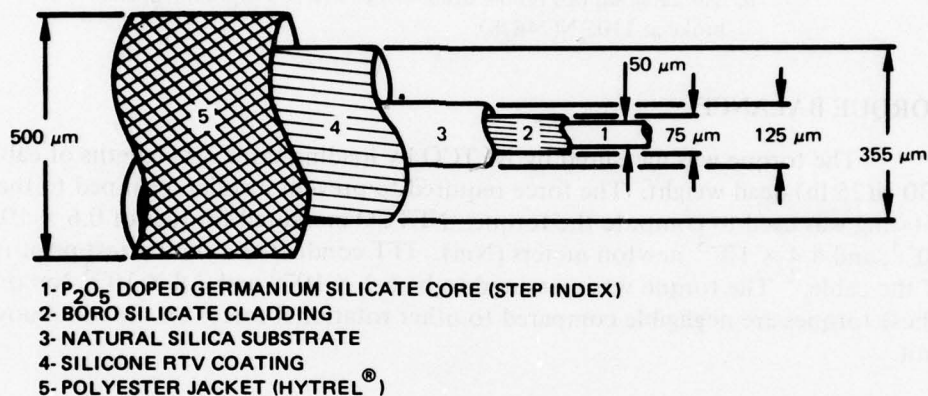


Figure 7. Five-km step-index optical fiber.

Table 5. ITT manufacturing data for 5-km step index fiber.

Fiber identification	SCVD 10480 - 110477 DEL-5
Primary coating	Silicone RTV Sylgard® 184
Secondary jacket	Hytrel®
Fiber length	5.430 km
Fiber diameter at start of draw, $\mu\text{m}$	132
Fiber diameter at end of draw, $\mu\text{m}$	130
Core diameter at end of draw, $\mu\text{m}$	52
NA	0.28
Attenuation @ .85 $\mu\text{m}$ , dB/km	
Before proof test	4.19
After proof test	4.16
Proof test, GPa (% elongation)	0.69 (1)

### Attenuation

Figure 8 shows the optical attenuation as a function of wavelength as measured by NOSC. The NOSC and ITT attenuation measurements agree within the 0.04 dB/km precision.

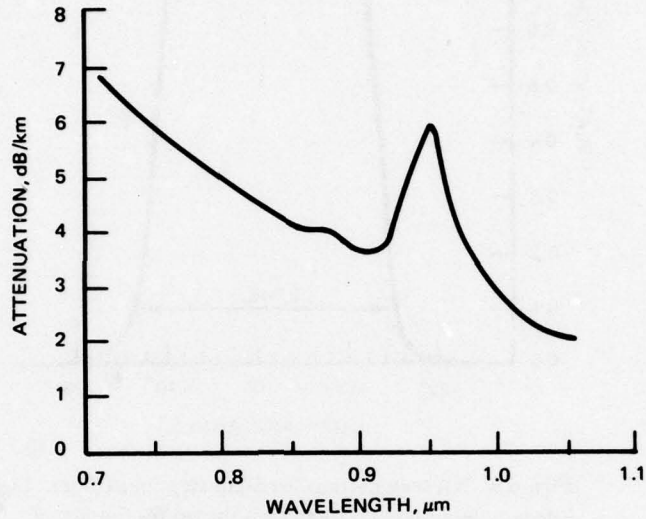


Figure 8. Five-km step-index optical fiber attenuation. The launch numerical aperture was 0.1 and the precision was  $\pm 0.04$  dB/km.

### Numerical Aperture

Numerical aperture measurements were made on the fiber by ITT using the visual method described in the cable numerical aperture section of this report and by NOSC using the far field scan method described in the same section. Table 6 lists the numerical apertures measured, figure 9 shows the scan pattern obtained for the 5.4-km length. The goal was 0.23 NA (min.), measured through 5 km using the scan method. The measured NA was 0.25.

Table 6. Step index numerical apertures.

Measured by	Length (m)	Method	NA
ITT	1	Visual	0.28
NOSC	1	Scan	0.267
NOSC	5400	Scan	0.246

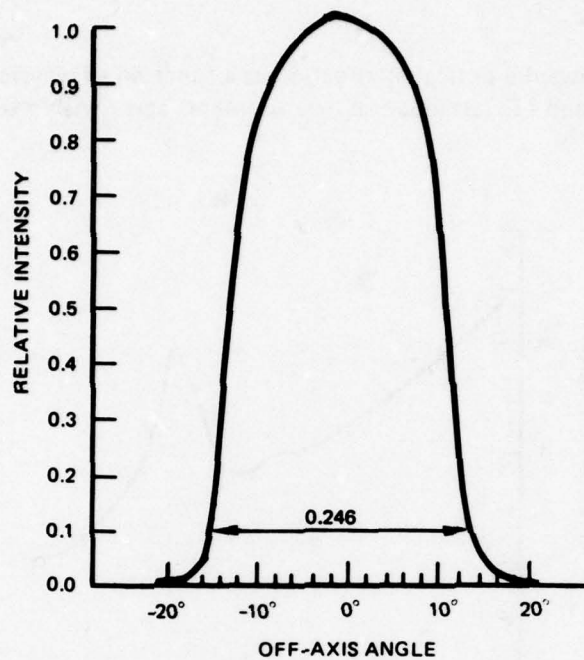


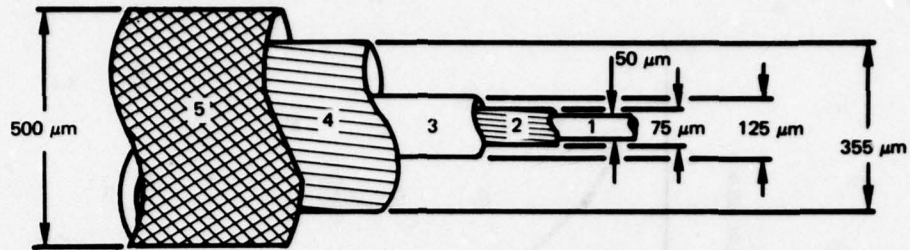
Figure 9. NA scan pattern for 5-km step index fiber. Light intensity as a function of angle is shown for 5.4 km of optical fiber (white light source).

#### HIGH STRENGTH 5-km GRADED-INDEX FIBER DEVELOPMENT

ITT also developed a 5-km graded index fiber under contract N66001-77-C-0137;<sup>5</sup> funds were provided by the Naval Material Command Fiber Optics Technology Development Program. The goals were 6 dB/km attenuation, 1 ns/km dispersion, 0.23 NA, 40  $\mu\text{m}$  core, and 1% elongation proof test. The fiber met all goals except numerical aperture (0.19 NA).

The preform diameter, material, and strength issues had been solved previously with the development of the step-index fiber. The remaining task was to adjust deposition parameters on the larger preform to produce low attenuation and dispersion. Based on the results of electron microprobe analysis of the dopant concentrations in the fiber cores, the refractive index profile was modified, yielding fibers which surpassed the contract goals for attenuation, dispersion, and core size. The resulting fiber, figure 10, was delivered to NOSC. ITT's manufacturing data is listed in table 7. The spectral attenuation curve is presented in figure 11. The NOSC and ITT spectral attenuation measurements agree within the 0.04 dB/km precision. The launch NA was 0.124. ITT measured dispersion using a pulsed injection laser; the 0.5-ns pulse width increased to 5.9 ns over the 5.25-km length. The numerical aperture was measured at NOSC using the far-field scan method. Results are listed in table 8 and figure 12.

This development removed the fiber-length limitation in fiber-optic cables for deep sonobuoy applications. The cabling techniques used in the fabrication of the prototype 1 km-length Kevlar-strengthened cable are conventional and do not pose any known limitation to the achievement of a 5-km cable. The remaining technical barriers are the demonstration



- 1- BORO SILICATE CORE DOPED WITH  $P_2O_5$  AND GRADED WITH  $GeO_2$
- 2- BORO SILICATE CLADDING DOPED WITH  $P_2O_5$
- 3- NATURAL SILICA SUBSTRATE
- 4- SILICONE RTV COATING
- 5- EXTRUDED POLYESTER JACKET (HYTREL®)

Figure 10. Five-km graded-index optical fiber.

Table 7. ITT manufacturing data for 5-km graded index fiber.

Fiber Identification	SCVD 10,580 022278 (DE)-4
Primary Coating	Silicone RTV Sylgard 184
Secondary Jacket	Hytrell
Fiber Length, km	5.252
Fiber Diameter at Start of Draw, $\mu m$	149
Fiber Diameter at End of Draw, $\mu m$	130
Core Diameter at End of Draw, $\mu m$	50
NA (1 m)	0.21
Dispersion, at 3 dB, ns/km	1.11
Attenuation @ 0.85 $\mu m$ , dB/km	
Before proof test	3.74
After proof test	3.49
Proof test, GPa (% elongation)	0.69 (1)

Table 8. Graded index fiber numerical aperture.

Measured by	Length (m)	Method	NA
ITT	1	Visual	0.21
NOSC	1	Scan	0.208
NOSC	5200	Scan	0.194

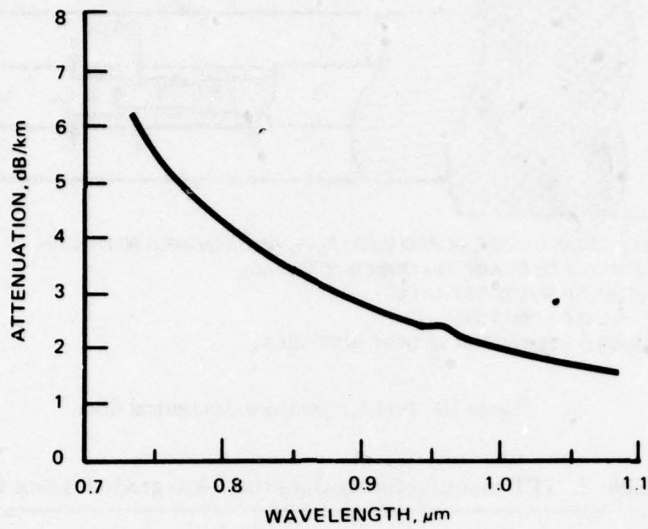


Figure 11. Five-km graded-index optical fiber attenuation. Attenuation as a function of wavelength is shown for the 5.2-km fiber. The launch numerical aperture was 0.12 and the precision was  $\pm 0.04$  dB/km.

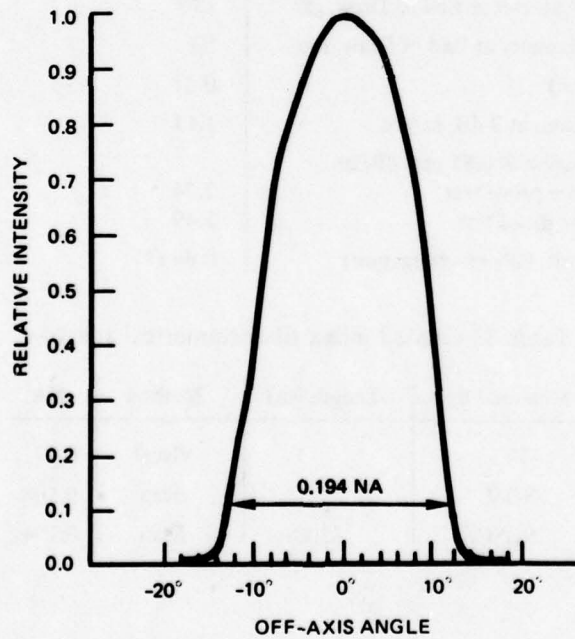


Figure 12. NA scan pattern for 5-km graded-index optical fiber. Light intensity as a function of angle is shown for 5.2 km of optical fiber (white light source).

of a low-cost duplex communication link and the improvement in fiber strength to the 2-3% proof test elongation level.

### TRIPLE-CORE FIBER FOR DUPLEX COMMUNICATION

ITT/EOPD developed and fabricated fiber having three optical cores as part of the sonobuoy cable contract (N00123-77-C-0079). The goal was to provide duplex communication using two separate optical cores (the third core, provided to improve fiber roundness, could be a spare), thereby eliminating the need for duplex couplers: the cores could be coupled to LEDs and detectors by small pigtail fibers. By use of a single triple-core fiber of the same buffered diameter as a single-core fiber, the same high-strength sonobuoy cable design could be used for duplex communication.

ITT's approach was to collapse a silica substrate tube about three conventional preforms. The resulting three-core preform was drawn into a 200- $\mu\text{m}$  diameter fiber, which was buffered and jacketed to 700  $\mu\text{m}$ . The cores were oblong with dimensions of 45  $\times$  63  $\mu\text{m}$ ; the fiber was slightly triangular and the center was incompletely collapsed, leaving a small, triangular void (see figure 13). The 600-m fiber was proof-tested to 1.4 GPa (2% elongation) and 100 m of it was cabled, using the single-core Kevlar cable design.

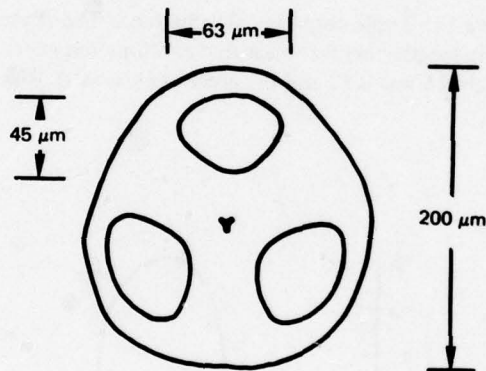


Figure 13. Cross-section of triple-core optical fiber.

The spectral attenuation (figure 14) and numerical aperture (figure 15 and table 9) of each of the cores were measured at NOSC.

### CABLED FIBER STRENGTH REQUIREMENT

Based on the results of the Kevlar sonobuoy cable tests in which the fiber strain was measured as function of cable tension, the fiber must withstand a momentary strain of 1.2% (cable peak dynamic load is 556 N(125 lb)), followed by a 3-hour strain of at least 0.9% (cable operating load is 330 N(75 lb)). The fracture mechanics model for static fatigue in glass<sup>6</sup> yields an equation for time to failure of the form

6. Wiederhorn, S. M.; Evans, A. G.; Fuller, E. R.; and Johnson, H.; J. Am. Ceram. Soc., 57, 319 (1974).

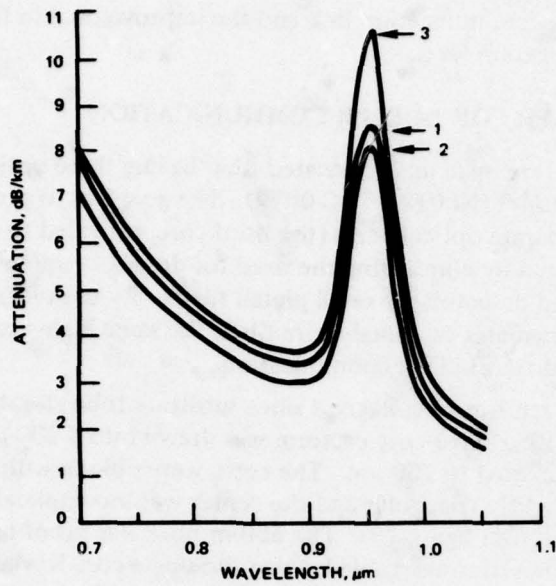


Figure 14. Triple-core fiber attenuations. The attenuation of a 500-m length fiber was measured as a function of wavelength. The launch NA was 0.12 and the precision was  $\pm 0.4$  dB/km.

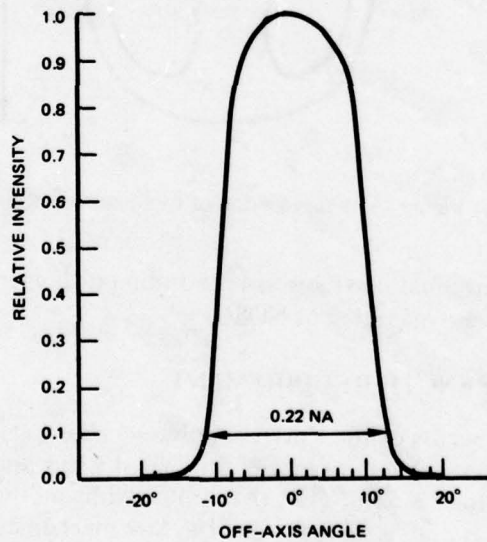


Figure 15. NA scan pattern for triple-core fiber (core 1). The numerical apertures of the three cores were measured using a  $0.85 \mu\text{m}$  source (500-m length). The NAs of the other two cores were each 0.21.

Table 9. Triple-core fiber numerical aperture.

Measured by	Length (m)	Method	Core 1	Core 2	Core 3
NOSC	1	Scan	0.25	0.24	0.24
NOSC	500	Scan	0.22	0.21	0.21

$$t_{\min} = B(\sigma_p)^{N-2} \sigma_A^{-N} \quad (2)$$

where  $t_{\min}$  = minimum time to failure

$B$  = a constant

$\sigma_p$  = proof test stress

$\sigma_A$  = applied stress

$N$  = fatigue parameter

The constants in eq 2 were evaluated<sup>7</sup> for ITT optical fibers in 23°C, 55% relative humidity atmosphere:  $B = 1.56 \times 10^6 \text{ MPa}^2\text{-sec}$  and  $N = 22.23$ . Substitution of these parameters into the equation gives a minimum proof test strain of 1.4% (for 8-hr life at 0.9% strain).\* This proof test level has been reported to have been exceeded (1.5% in 6 km) in the laboratory.\*\*

#### FIBER STRENGTH IMPROVEMENT PROGRAM

A development effort, funded by Defense Advanced Research Projects Agency (DARPA) through 1978 and by Naval Material Command (NAVMAT) in 1979 and beyond, has the goal of developing 10-km fibers that can withstand 2-3% proof test strain and which do not fatigue significantly over 5-year operating lives. The participants are Hughes Research Laboratories (HRL), Catholic University of America (CUA), ITT/EOPD, and Gulf and Western/Galileo (GW/G). Contracts in the DARPA/NAVMAT strength-improvement program are detailed in the following paragraphs.

#### HRL Contract

HRL is funded through April 1979 under contract 77G-102280-000 to complete work on preserving pristine fiber strength by hermetically sealing the fiber with a thin layer

7. Ritter, J. E., Jr.; Sullivan, J. M., Jr.; and Jakus, Karl; Application of Fracture-Mechanics Theory to Fatigue Failure of Optical Glass Fibers *J. Appl. Physics*, 49(9), 4779, September 1978.

\*Dynamic and static fatigue tests of Bell Laboratories optical fibers<sup>8</sup> yielded a value of 20 for  $N$ .

\*\*Adolph Asam, ITT Electro-Optical Products Division, private communication, unpublished data.

8. Schonhorn, H.; Wang, T. T.; Vazirani, H. N.; and Frisch, H. L.; Static and Dynamic Fatigue of High-Strength Glass Fibers Coated with UV-curable Epoxy-Acrylate, *J. Applied Physics*, 49(9), 4783 September 1978.

of metal. Aluminum was applied in 10  $\mu\text{m}$  thick dip-coatings to optical fibers as they were drawn. Areas still under investigation are

- (a) nonuniformity in the adherence of the metal to the fiber
- (b) flaking and fatigue of the metal coating when the fiber is subjected to low-tension cyclic loading
- (c) increased fiber attenuation due to metalizing the fiber.

HRL has drawn metalized fibers 1 km in length having attenuation of approximately 11 dB/km at 0.85  $\mu\text{m}$ . The metal coating did not introduce excess loss when the fiber was in a strung condition. When a fiber was subjected to a 0.6% strain, its attenuation increased 8.5 dB/km for one cycle of loading and 10 dB/km for 3 cycles.

#### **CUA Contract**

CUA has completed the investigation of Phasil-stuffed fibers having compressive claddings under contract F19628-77-C-0084. They have fabricated rods capable of producing fibers having 410 MPa(60 kpsi) compression in the cladding. The effect of compressive claddings is to prevent failure of fibers at stresses less than the compression level.

#### **ITT Contracts**

ITT completed the DARPA-funded contract 12720 (62-657-60131) 76R to perfect processing methods to improve pristine fiber strength. Fibers can now be routinely proof-tested to 1% strain in 5-km lengths. They are currently being awarded a contract (N00123-79-C-0301) by NOSC (NAVMAT funding) to investigate and demonstrate a method of incorporating residual surface compression in a modified chemical vapor deposition (MCVD) processed fiber. A goal is to use the same machinery previously used in the high strength program funded by DARPA. The compression goal is greater than 690 MPa (100 kpsi).

#### **Gulf and Western/Galileo Contract**

Plasma deposition of metal or dielectric in a vacuum on pristine fibers is currently being investigated under contract F19628-78-C-0180 by these companies jointly under DARPA/Air Force funding. The fiber will be precoated to several angstrom thickness by the plasma method to provide a base for uniform coating to several micrometers thickness when the fiber is drawn through a molten bead (a dip coat) of the same coating material.

#### **NOSC Tests of High-strength Fibers**

The DARPA-funded NOSC testing facility received fibers from the ITT (processing improvement) and HRL contracts. The plastic-coated ITT fiber had been proof tested at ITT to 3% strain over its 2-km length. Short-length (60-cm gage length) tests at NOSC of the ITT fiber showed a unimodal flaw distribution indicating that flaws of the size characteristic of poor processing (bubbles, inclusions, surface contamination, and abrasion) had been eliminated. In a water-immersion test, the plastic coating was penetrated by distilled water in 15 minutes and saturated in 30 minutes. Dynamic fatigue tests, in which the strengths

of short-length samples were measured as a function of strain rate, revealed that the plastic-coated fibers exhibited the normal stress-corrosion of uncoated glass in a humid environment.

The HRL metal-coated fibers were dynamically tested in water over the same strain rate range as the ITT fibers. There was no change in average breaking strength as a function of strain rate, indicating that the metal-coated fibers did not fatigue in the presence of water.

### Summary of Strength Improvement Program

High pristine fiber strength (at least 1.5% strain in 6-km lengths) has been achieved. Plastic coated fibers, with strengths sufficient to achieve 3-hour operation at 0.9% strain are attainable, meeting minimum sonobuoy cable requirements. If the identified problems with the hermetic sealing approaches are removed, the resistance to fatigue of the metal-coated fibers could provide considerable safety margin (1.7 to 1) during operation in the seawater environment. Compressive claddings, if successful, may also provide safety margin by preventing slow crack growth indefinitely at operating stresses less than the compressive stress.

## 5-km LINK DEMONSTRATION

### INTRODUCTION

The goal of the demonstration was to transmit 50 kb/s data over a 5-km fiber optic link (see figure 16) with sufficient optical power to accommodate optical losses associated with connectors, fiber attenuation, splices and duplex couplers. Commercially-available LEDs, a 5-km optical fiber, and a NOSC-developed optical receiver were assembled into a laboratory link. It was concluded that a fiber optic duplex link for a deep sonobuoy would be feasible with available technology. The fiber bandwidth is more than two orders of magnitude greater than the data requirement of the sonobuoy (50 kb/s).

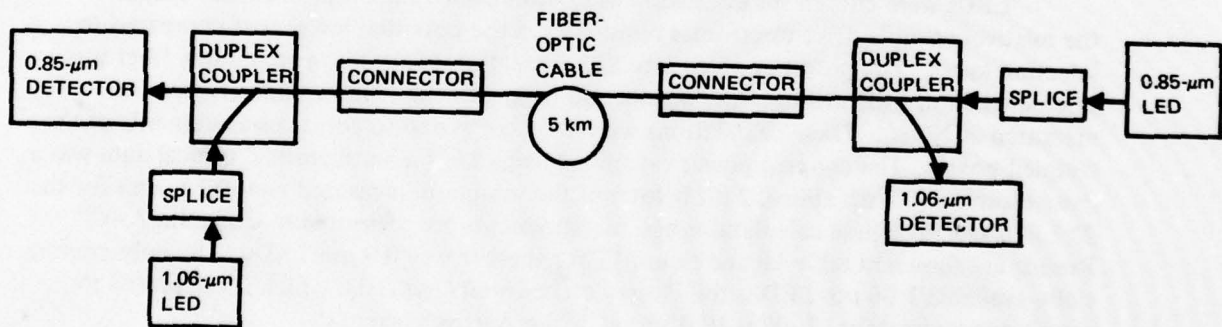


Figure 16. Sonobuoy duplex link schematic.

## OPTICAL POWER PERFORMANCE

### Link Power Margin

The link power margin, equation (3), is the difference between the available optical power (in dBm) coupled into a fiber by the optical source and that required to assure reliable link transmission:

$$P_m = P_c + L_f + L_c + L_s + L_D - P_D \quad (3)$$

where

$P_m$  = link power margin, dB

$P_c$  = average power coupled into fiber, dBm

$L_f$  = fiber attenuation, \* dB

$L_c$  = connector insertion loss, \* dB

$L_s$  = splice insertion loss, \* dB

$L_D$  = duplex coupler insertion loss, \* dB

$P_D$  = minimum average power at detector for specified error rate, dBm

Each term in equation (3) will be discussed in the following paragraphs with respect to a 5-km bidirectional link operating at 0.85  $\mu\text{m}$  and 1.06  $\mu\text{m}$ . An example of a link margin calculation will be presented at the conclusion of the discussion, using the values measured at NOSC for the LED, fiber, and detector; insertion losses for typical connectors, splices, and duplex couplers will be assumed for the calculation.

### LED Coupled Power

LEDs were chosen for evaluation as candidates for the optical source because of the relatively simple drive electronics required and the potential lower cost compared to injection lasers. The power coupled into a short section of the 5-km step-index fiber was calculated from LED manufacturers' data and from LED emission characteristics data measured at NOSC. These calculations were then compared to actual measurements of the coupled power. The coupled power calculated using LED manufacturers' typical data was a good estimate (0.2 dB above, 2 dB below) of the minimum measured coupled power for the 23 LEDs tested. These calculations and measurements are presented in appendix A-C. Results are shown in table 10 and figure 17 for these 0.8 to 0.9  $\mu\text{m}$  LEDs. The only commercially-available 1.06  $\mu\text{m}$  LED is the Plessey etched-well GAL-103, which is calculated to couple approximately 12  $\mu\text{W}$  (-19 dBm) at 150 mA drive current.

### Fiber Attenuation

The attenuation of the optical fiber in the sonobuoy cable (figure 2) represented the state of the art in cabled fiber attenuation in 1977. Subsequent progress in the development of 5-km optical fibers has resulted in lower attenuation. For purposes of estimating the link

\*Losses are defined as  $10 \log (P_{\text{out}}/P_{\text{in}})$ ;  $L_f, L_c, L_s, L_D$  are negative numbers.

Table 10. LED coupled power,  $P_c$ , into a fiber. (a)

ID	Type	$\lambda_{\text{Peak}}$ $\mu\text{m}$	Typ $P_c^{(b)}$ $\mu\text{W}$	Min. (c) Est. $P_c$ $\mu\text{W}$	Min. (d) Meas. $P_c$ $\mu\text{W}$
A	Etched well	0.82	96.0	(e)	50.3
B	Edge emitter	0.85	5.2	9.4	8.3
C	Edge emitter	0.83	3.7	3.2	3.7
D	GaAs laser	0.90	2.4	3.1	2.3
E	GaAs laser	0.90	2.4	2.4	3.1
F	GaAs laser	0.90	3.2	3.6	4.0
G	AlGaAs laser	0.86	4.0	4.6	6.0
H	AlGaAs laser	0.85	2.4	2.6	3.0
I	GaAs surface	0.90	0.5	0.7	0.4

- a. Drive current 100 mA; 23 LEDs tested
- b. Calculated from manufacturer's data for typical LEDs
- c. Calculated from measured emission characteristics (appendix A), min.  $P_c$  in each LED group
- d. Measured power coupled into 0.26 NA, 52  $\mu\text{m}$  core fiber, min.  $P_c$  in each LED group
- e. Not measured; LED was supplied with fiber attached

power margin, the worst-case curve shown in figure 2 is assumed; -25 dB total (for 5 km of cable) at 0.85  $\mu\text{m}$  and -12 dB total at 1.06  $\mu\text{m}$  for  $L_f$ . If the fiber attenuation shown in figure 11 were used, the attenuation would be 7 dB less at 0.85  $\mu\text{m}$  and 3 dB less at 1.06  $\mu\text{m}$ .

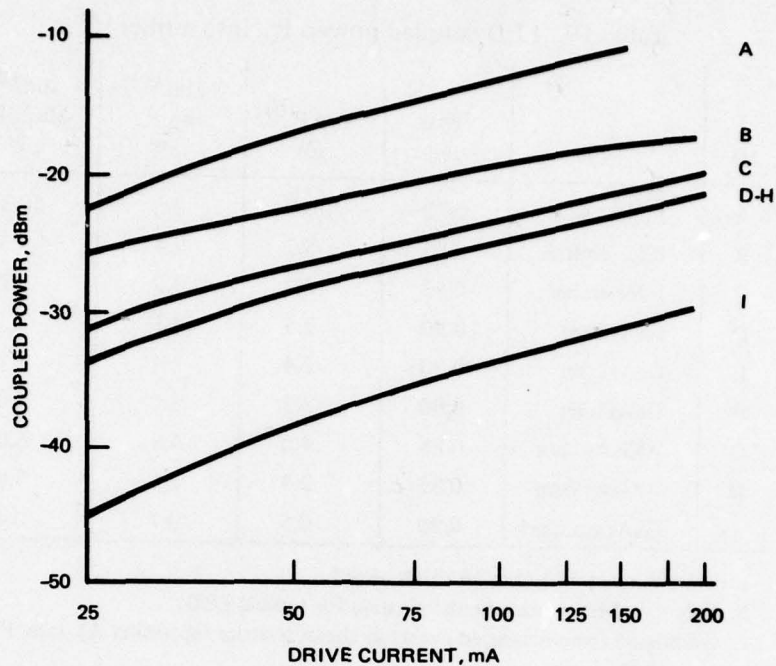
### Connectors

Single-fiber connectors are available commercially from several manufacturers for land-based installations. Connectors that can operate at pressures up to 50 MPa (7 kpsi) as pressure penetrators or as pressure-compensated connectors are not available and must be developed. For purposes of estimating the link power margin, an insertion loss of -1 dB at each end of the cable will be assumed for  $L_c$ .

### Duplex Couplers and Splices

Wavelength-selective directional couplers for two-way transmission are now commercially available which have -1.5 dB insertion loss at 0.85  $\mu\text{m}$  and -3 dB at 1.06  $\mu\text{m}$ ; crosstalk is 40 dB at both wavelengths.<sup>9</sup> Additional crosstalk reduction can be achieved by filtering each detector to reduce the interfering signals to at least -11 dB below the desired signals (at the detectors). The power penalty for a low-pass or high-pass filter is approximately -1 dB, making  $L_D$  equal to -4 dB at 0.85  $\mu\text{m}$  and -7 dB at 1.06  $\mu\text{m}$ . An additional power loss of -1 dB will be assumed for splicing losses,  $L_s$ , between the pigtails of the LED and duplex coupler.

9. ITT Data Sheet, "Optical Fiber Couplers."



- A. ETCHED-WELL LED
- B-C. EDGE-EMITTER LED
- D-H. INJECTION LASERS USED AS LEDs
- I. SURFACE EMITTER LED

Figure 17. Measured coupled powers for 0.8 to 0.9  $\mu\text{m}$  LEDs as a function of drive current. 23 LEDs were evaluated; the data was plotted for representative LEDs in each group. The fiber was a 2-meter section of the 5-km step-index optical fiber (0.26 input NA, 52  $\mu\text{m}$  core diameter).

### Receiver Required Optical Power

An optical receiver constructed at NOSC was optimized for operation at 0.85  $\mu\text{m}$  at 50 kb/s data rate.<sup>3</sup>

The receiver was tested for bit error rate (BER) as a function of average optical power at the detector. A BER tester, Tau-Tron Model PTS-107, was used to generate and detect a 9-bit pseudorandom noise (PRN) sequence of non-return-to-zero (NRZ) pulses with a clock rate of 45 kHz. The clock for the receiver section of the BER tester was provided internally. The optical source was an RCA SG2001 LED, driven by one stage of a hex inverter. The power,  $P_c$ , coupled through the 5-km step-index fiber was measured, using a United Detector Technology Model 111A radiometer. The measured data and calculated values are presented in figure 18. Note that a 1.2-dB increase in optical power changes the BER by 3 orders of magnitude. At the 45-kHz clock rate, a  $10^{-8}$  BER corresponds to one error in approximately one-half hour. This test demonstrates that average power,  $P_D$ , required for reliable detection of digital data is -68 dBm (160 pW) at 0.85  $\mu\text{m}$ .

The performance of the receiver at 1.06  $\mu\text{m}$  was estimated to be approximately 5 dB less sensitive than at 0.85  $\mu\text{m}$ , or -63 dBm required average optical power (appendix D).

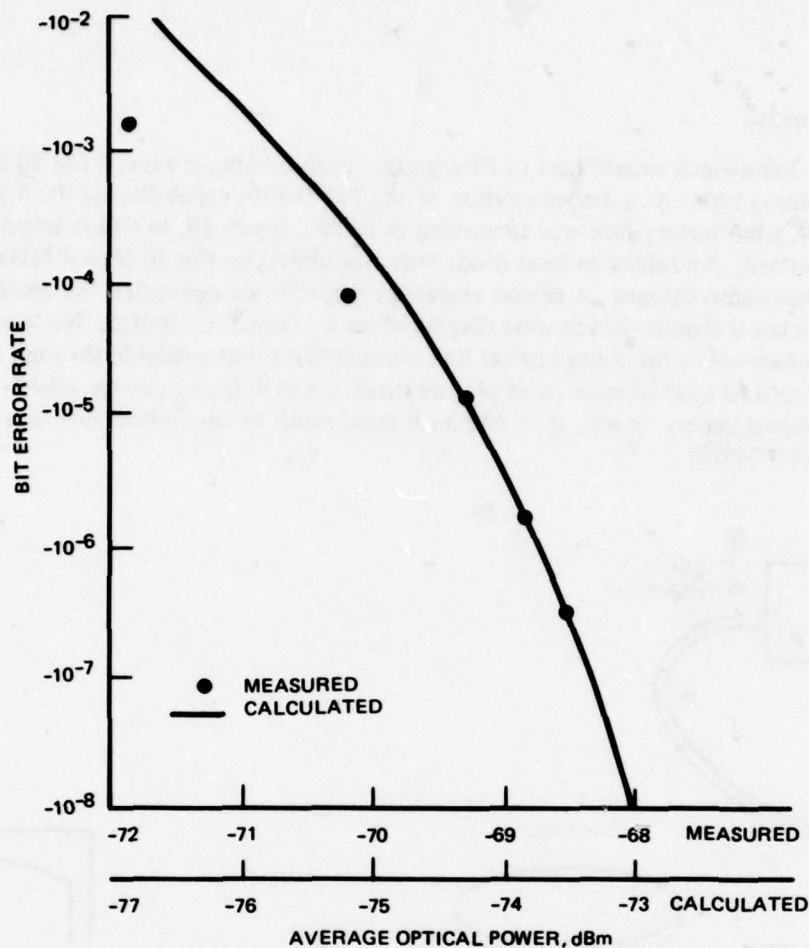


Figure 18. NOSC receiver sensitivity.

### LINK PERFORMANCE ESTIMATE

In order to determine the minimum acceptable LED coupled power,  $P_c$ , let the link margin,  $P_m$ , be zero and solve equation (3) for  $P_c$ .

$$P_c = P_D - (L_f + L_c + L_s + L_D) \quad (4)$$

Substitution of values discussed in the previous paragraphs yields a minimum  $P_c$  of -36 dBm at 0.85  $\mu\text{m}$ . From figure 17, this coupled power level at 0.8 to 0.9  $\mu\text{m}$  was achieved or exceeded by all edge-emitter and etched-well LEDs measured (for drive currents exceeding 25 mA). For example, the power margin for the LED B edge emitter was 18 dB at 150 mA drive current.

The minimum required coupled power at 1.06  $\mu\text{m}$  is -41 dBm. The Plessey LED couples -19 dBm at 150 mA, yielding a link margin of 22 dB.

From these performance estimates it is concluded that a bidirectional fiber-optic link for deep sonobuoys is feasible with available technology.

### Fiber Bandwidth

The bandwidth capabilities of fiber-optic components far exceed the 50 kb/s required of the sonobuoy link. As a demonstration of the bandwidth capability of the 5-km step-index optical fiber, a laboratory link was assembled at NOSC, figure 19, in which television signals were transmitted. An injection laser diode was modulated by the 20 Hz - 4 MHz analog video signal of a television camera. A silicon avalanche photodiode converted the received optical signal to electrical signals, which were displayed on a television monitor. No loss of resolution was observed in the 5-km optical link compared to that available through a short length of electrical coaxial cable, and picture quality was judged to be excellent. In a test in which a signal generator was used, the 3-dB bandwidth of the optical link was measured to be at least 10 MHz.

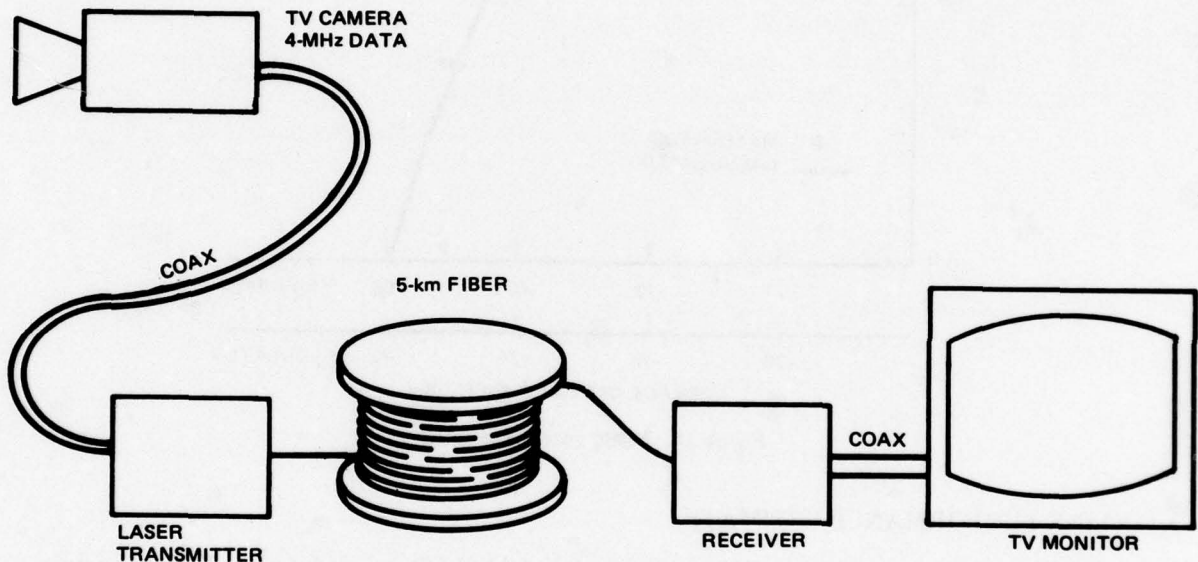


Figure 19. Five-km wideband link demonstration.

### CONCLUSIONS

1. CABLES. Test results of the 1-km sample fiber-optic sonobuoy cable indicate that a cable that meets the mechanical and environmental specifications of a 5-km depth sonobuoy can be fabricated. The specific problems identified in the previously developed steel-strength member cable were solved by the development of the Kevlar cable:

(a) Attenuation increases from factors such as temperature, tension, and bending were virtually eliminated by increasing the fiber NA from 0.24 to 0.30, changing the buffer jacket from PFA (which contained lumps) to Hytrel, increasing buffered fiber diameter from 0.5 mm to 0.7 mm, and moving the fiber from the edge of the cable to the center of the cable (one fiber, surrounded by contrahelical Kevlar elements).

(b) Attenuation increases resulting from high hydrostatic pressure were eliminated by removing the outer jacket, allowing the water to flood the cable.

(c) The steel cable was not torque balanced because of the twisted construction, which caused the cable to rotate under load. Torque balance was obtained by using contra-helical Kevlar layers.

(d) The steel cable had a diamond-shaped cross section, making it difficult to wind in a cable pack. The coaxial design of the Kevlar cable yields a circular, easily-wound cable.

(e) The steel cable weighed 190 N (42 lb) in 5-km lengths, which decreased the load-carrying capability of the cable. The weight problem was eliminated by using Kevlar as the strength member, which reduced the in-water weight to 22 N (5 lb).

2. FIBERS. Optical fibers can be fabricated in the required length, strength, and optical properties. Development of the 5-km fibers removed the fiber-length limitation in fiber-optic cables for deep sonobuoy applications. The cabling techniques used in the fabrication of the sample 1-km-length Kevlar-strengthened cable are conventional and do not pose any known limitation to the achievement of a 5-km cable.

Fibers having three optical cores to allow bidirectional communication were demonstrated. Attenuation was approximately 4 dB/km at 0.85  $\mu\text{m}$ .

The DARPA/NAVMAT fiber strength improvement program has provided the technical foundation at ITT for drawing strong optical fibers capable of withstanding proof tests as high as 1.5% strain in 6-km lengths. This fiber strength is required for an 8-hr sonobuoy life at the operating strain of 0.9%.

Prevention of fiber-strength degradation under load by use of metal hermetic seals is possible, but the aluminum dip-coating approach used by HRL resulted in excess attenuation under load and work-hardening of the metal in cyclic loading tests.

Compressive claddings exhibiting 0.4 GPa (60 kpsi) of compression have been demonstrated in Phasil-stuffed fibers by Catholic University.

3. LED COUPLED POWER. The calculations (appendix A) and measurements performed at NOSC indicate that the variability of the LEDs is significant (as much as 4-dB range in coupled power for one group of LEDs tested), which makes estimates based on manufacturers' data unreliable. For the LEDs tested, the estimated coupled power (derived from manufacturers' data for typical LEDs) was approximately equal to the minimum measured coupled power in each group. It is possible to calculate the power coupled into an optical fiber within typically  $\pm 0.8$  dB of the measured value if the emission characteristics of the individual LED are measured.

4. RECEIVER PERFORMANCE. Test results of the 50 kb/s optical receiver designed and fabricated at NOSC indicate that an optical receiver can be fabricated that is 11 dB more sensitive than the best known laboratory receiver (1.5 Mb/s data rate, PIN detector),<sup>10</sup> and within 5 dB of theory. This was accomplished by optimizing the receiver bandwidth for 50 kb/s data. It achieved a  $10^{-8}$  BER for -68 dBm average power at 0.85  $\mu\text{m}$  wavelength for NRZ-PRN data at 45-kHz clock rate. Its performance at 1.06  $\mu\text{m}$  was calculated to be 5 dB less sensitive than at 0.85  $\mu\text{m}$ .

10. Muska, W. M., An Experimental Optical Fiber Link for Low-Bit-Rate Application, BSTJ 56, No 1, 65, January 1977.

5. **OPTICAL LINK POWER MARGIN.** Tests of a link consisting of an AlGaAs edge emitter LED (0.85  $\mu\text{m}$  wavelength, 150 mA drive current), the 5-km step-index optical fiber, and the NOSC receiver showed that, when the estimated losses for the other link components such as duplexers, connectors and splices are included, there is sufficient optical power available (18 dB margin) with present components to meet deep sonobuoy data link transmission requirements.

### RECOMMENDATIONS

1. Verify the sonobuoy cable operational capability by measuring the change in attenuation under load in a water environment.
2. Continue to improve fiber pristine strength and durability. In order to achieve the same 4:1 strength safety margin as the cable, the fiber must have an initial elongation capability of 2.5%, with minimal degradation during a 3-hour operating life.
3. Evaluate available bidirectional (duplex) couplers and modify, as necessary, for deep sonobuoy.
4. Support development of long-wavelength (1.0 to 1.3  $\mu\text{m}$ ) LEDs and detectors in order to utilize the lower attenuation of optical fibers at long wavelengths and to provide another wavelength for duplex transmission.
5. When purchasing LEDs, specify minimum coupled power out of a user-specified fiber pigtail which is identical to the cabled fiber. This approach removes coupling uncertainties associated with LED emission characteristics such as fiber misalignment, side-light and Fresnel losses.
6. Establish a technique for reliably splicing optical fiber pigtails to the optical components of the link.
7. Standardize LED emitted power specifications for fiber optic applications. Manufacturers of LEDs should specify, as a minimum, the power coupled into representative commercially-available fibers, giving details of fiber core size, index profile, and numerical aperture. In order for designers of fiber-optic systems to estimate the performance of various LEDs in specific applications, it is further recommended that LED data sheets include the LED emitting area and emitted power as a function of drive current and detector solid angle (excluding contributions from side light in edge emitters). A recommended measurement device, which provides such data, is a micro-radiometer: a lens of variable NA images the LED emitting area onto a variable aperture adjacent to the detector. This method eliminates the contributions from the edge-emitter side light.

Although not discussed in this report, several tasks remain in the transitioning of fiber optics from the laboratory to an advanced system. These tasks relate to mechanical engineering aspects associated with buoy design and deployment.

1. Purchase additional cable (1-2 km) and develop winding and payout techniques to assure minimum optical attenuation in the coiled configuration and to prevent fouling or fiber breakage during payout.
2. Develop a cable braking method to deploy the sensor to preprogrammed depths.
3. Investigate compliant members to provide the cable with wave-motion isolation.

4. Investigate the pressure-tolerance of electro-optical components, such as LEDs, photodiodes, and duplexers to assure compatibility with pressure-tolerant buoy designs.

5. Develop a fiber-optic feedthrough technique to provide reliable optical penetration of the pressure housing. Develop fiber-optic undersea connectors capable of withstanding 48 MPa (7 kpsi) pressure.

#### REFERENCES

1. NOSC TR 148, "Fiber Optic Sonobuoy Cable Development FY76," by R. A. Eastley, 8 August 1977.
2. NOSC TR 297, "Fiber Optic Sonobuoy Cable Development FY77," by R. A. Eastley and W. H. Putnam, 15 August 1978.
3. Final Report, Contract N00123-77-C-0079, "Follow-on Development of Fiber Optic Cables for Sonobuoy Systems," 5 April 1978, ITT/EOPD.
4. DoD STD 1678 Fiber Optical Test Methods and Instrumentation.
5. NOSC contract N66001-77-C-0137, "Development and Fabrication of High Strength Long Length Optical Fiber," ITT/EOPD.
6. Wiederhorn, S. M.; Evans, A. G.; Fuller, E. R.; and Johnson, H.; J. Am. Ceram. Soc., 57, 319 (1974).
7. Ritter J. E., Jr; Sullivan, J. M., Jr; and Jakus, Karl, Application of Fracture-Mechanics Theory to Fatigue Failure of Optical Glass Fibers, J. Appl. Physics, 49(9), 4779, September 1978.
8. Schonhorn, H.; Wang, T. T.; Vazirani, H. N.; and Frisch, H. L., Static and Dynamic Fatigue of High-Strength Glass Fibers Coated with UV-curable Epoxy-Acrylate, J. Applied Physics, 49(9), 4783 September 1978.
9. ITT Data Sheet, "Optical Fiber Couplers."
10. Muska, W. M., An Experimental Optical Fiber Link for Low-Bit-Rate Application, BSTJ 56, No 1, 65, January 1977.
- D-1. Yariv, A., Introduction to Optical Electronics, 2nd Ed, 1976, Holt, Rinehart, Winston, 292, 331.
- D-2. Goell, J. E., An Optical Repeater with High-Impedance Input Amplifier, BSTJ 53, No. 4, 629, April 1974.

## APPENDIX A LED COUPLED POWER CALCULATION

The equation for coupled power is

$$P_c = P_T \eta_c \eta_\theta \eta_f \eta_s \quad (5)$$

where

$P_c$  = power coupled into fiber

$P_T$  = total power emitted by LED into a hemisphere

$\eta_c$  = fraction of total power in area equal to core area

$\eta_\theta$  = fraction of total power in fiber NA ( $\approx NA^2$ )

$\eta_f$  = fiber NA response correction factor = 0.56 (appendix B)

$\eta_s$  = LED side-light correction factor (appendix C)

The coupled power was calculated using both manufacturers' data sheets (missing data was obtained by telephone conversations with the LED manufacturers) and measurements of the far-field patterns (which were integrated to yield  $P_T$  and  $\eta_\theta$ ), emitting area (which were integrated to yield  $\eta_c$ ), and fiber NA scans (which were integrated to yield  $\eta_f$ ). The calculated and measured results are listed in table A-1 and figures A-1-A-3.

The calculations and measurements listed in table A-1 indicate that while it is possible to calculate the coupled power with typically 0.8-dB accuracy if the emission characteristics of the individual LED are known, the variability in emission characteristics of the individual LEDs is much greater: there was a 4-dBm range (3.7 to 9.1  $\mu$ W) between minimum and maximum coupled power for LED C. For initial design purposes, there is a much better fit between the estimated power (derived from manufacturer's data for typical LEDs) and the *minimum* measured power coupled into a short fiber: the minimum measured power of all LED types was within 2 dB above or 0.2 dB below the estimated value.

Table A-1. LED coupled power into a fiber.

ID	Type	$\lambda_{\text{peak}}$ $\mu\text{m}$	$P_T$ @ 100 mA			$P_c$	
			mW	$\eta_c$	$\eta_\theta$	calc. $\mu\text{W}$	meas. $\mu\text{W}$
Typ. A	Etched-well	0.82	3.5	1.0	0.07	96.0	(a)
A1	Etched-well	(b)	(b)	(b)	(b)	(b)	50.3
Typ. B	Edge emitter	0.85	0.50	0.35	0.080	5.2	(a)
B1	Edge emitter	0.80	0.66	0.40	0.092	9.1	11.8
B2	Edge emitter	0.81	0.78	0.52	0.084	12.8	13.8
B3	Edge emitter	0.84	1.20	0.35	0.060	9.4	8.3
B4	Edge emitter	0.83	1.14	0.35	0.055	8.2	8.8
Typ. C	Edge emitter	0.83	0.40	0.35	0.070	3.7	(a)
C1	Edge emitter	0.82	0.49	0.37	0.055	3.7	4.8
C2	Edge emitter	0.82	0.53	0.37	0.060	4.4	4.1
C3	Edge emitter	0.85	0.44	0.46	0.082	6.2	9.1
C4	Edge emitter	0.83	0.49	0.37	0.048	3.2	3.7
Typ. D	GaAs laser <sup>(c)</sup>	0.90	0.20	0.69	0.070	2.4	(a)
D1	GaAs laser	0.92	2.14	0.43	0.024	5.4	4.4
D2	GaAs laser	0.92	0.65	0.69	0.028	3.1	2.3
D3	GaAs laser	0.94	0.70	0.69	0.029	3.5	3.4
D4	GaAs laser	0.92	1.91	0.43	0.026	5.3	5.0
D5	GaAs laser	0.92	0.60	0.69	0.027	2.8	3.0
Typ. E	GaAs laser	0.90	0.20	0.69	0.07	2.4	(a)
E1	GaAs laser	0.93	1.06	0.69	0.026	4.7	4.1
E2	GaAs laser	0.92	0.49	0.74	0.033	2.4	3.1
E3	GaAs laser	0.91	2.13	0.76	0.022	8.8	5.4
E4	GaAs laser	0.93	0.91	0.69	0.030	4.6	4.4
E5	GaAs laser	0.92	0.91	0.69	0.025	3.9	2.9
Typ. F	GaAs laser	0.90	0.40	0.35	0.07	3.2	(a)
F1	GaAs laser	0.92	0.71	0.35	0.044	3.6	4.0
Typ. G	AlGaAs laser	0.85	0.50	0.35	0.07	4.0	(a)
G1	AlGaAs laser	0.86	0.79	0.35	0.05	4.6	6.0
Typ. H	AlGaAs laser	0.85	0.30	0.35	0.07	2.4	(a)
H1	AlGaAs laser	0.86	0.37	0.35	0.06	2.6	3.0
Typ. I	GaAs surface	0.90	0.18	0.07	0.07	0.5	(a)
I1	GaAs surface	0.91	0.15	0.11	0.07	0.7	0.4

(a) Calculated power derived from data sheet values for typical LEDs, supplemented by telephone conversations with LED manufacturers.

(b) Not measured. The LED was ordered with 3 meters of the 5-km step-index fiber attached.

(c) Broad-area single-heterojunction lasers operated below threshold as LEDs.

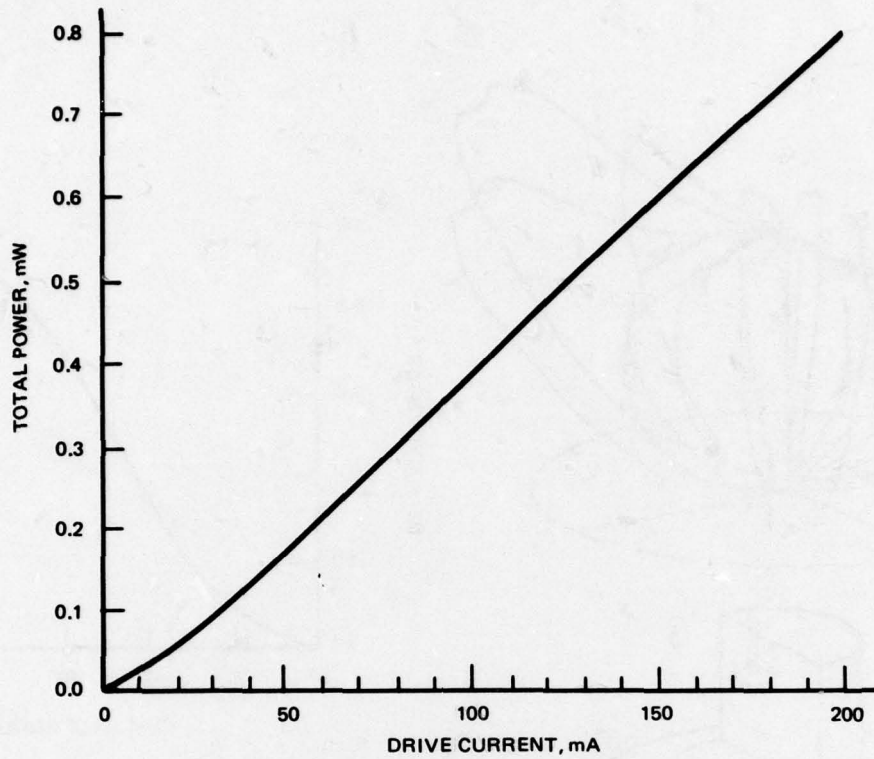


Figure A-1. Total power vs drive current for typical edge emitter LED. The total power was integrated from the far-field pattern at 50 mA. Relative power was measured as a function of drive current. The manufacturer's specification was 0.8 mW at 200 mA.

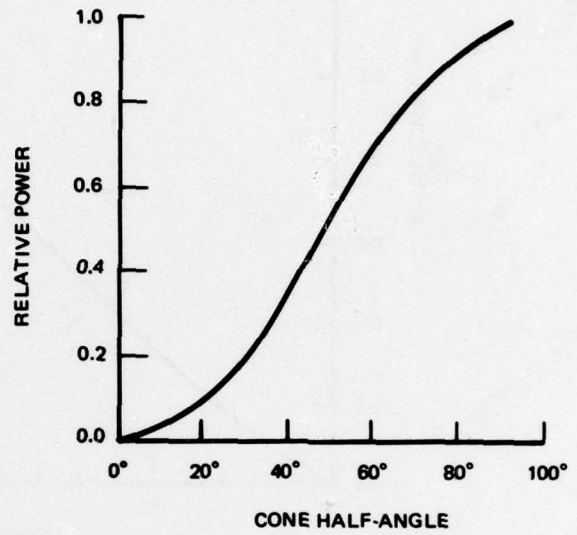
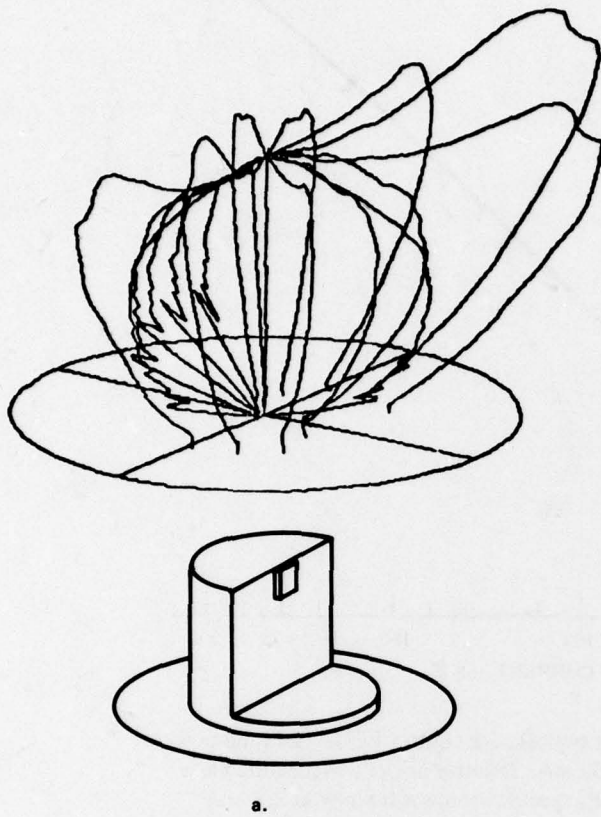


Figure A-2. Far-field pattern (angular distribution) of typical edge-emitter LED. a. Light is emitted from all four edges of the chip, causing strong sidelobes. b. The integrated power, as a function of cone angle, includes light from the sides of the chip (approximately 33% at the fiber NA angle of  $15.4^\circ$ ). The fraction of light available to the fiber is thus  $0.67 \times 0.055 = 0.037$ .

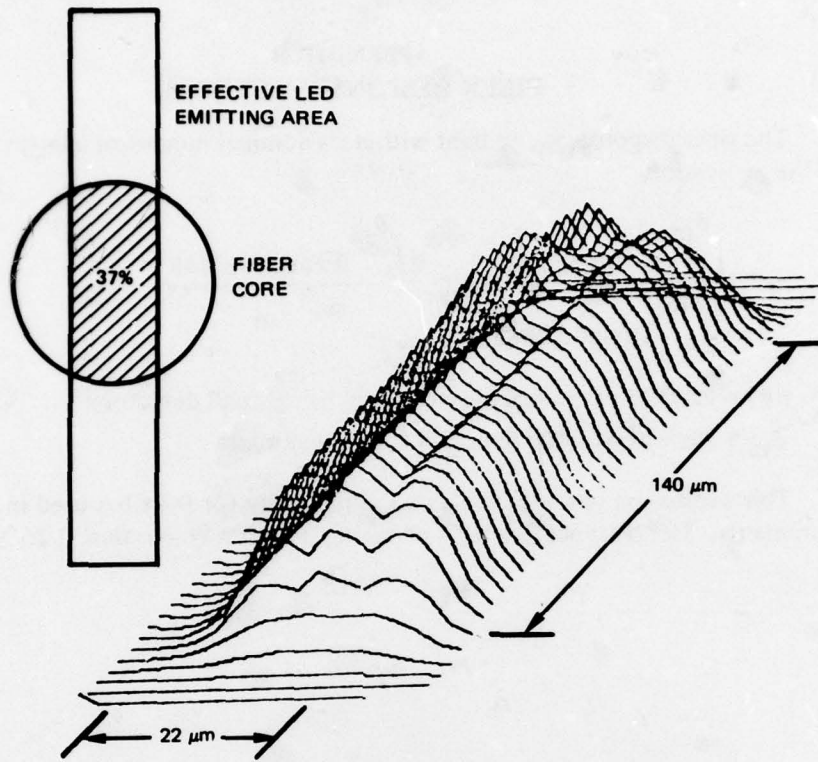


Figure A-3. Emitting area of typical edge-emitter LED. The light from the front edge of the LED is reasonably uniform; the effective dimensions of the emitting area are  $22\ \mu\text{m} \times 140\ \mu\text{m}$ . The  $52\ \mu\text{m}$  fiber core intercepts 37% of the light.

**APPENDIX B**  
**FIBER RESPONSE FACTOR,  $\eta_f$**

The fiber response,  $\eta_f$ , to light within its nominal numerical aperture can be calculated using the expression

$$\eta_f = \frac{\int_0^{\theta_m} f(\theta) 2\pi \sin\theta \cos\theta d\theta}{\int_0^{\theta_m} 2\pi \sin\theta \cos\theta d\theta} = 2 \int_0^{\theta_m} \frac{f(\theta) \sin\theta \cos\theta d\theta}{\sin^2 \theta_m} \quad (\text{B-1})$$

$f(\theta)$  = far-field numerical aperture scan using small detector

$\theta_m$  = angle at which intensity is 0.1 of maximum

This expression has been evaluated numerically for the fiber used in the LED coupling measurements. The fiber accepts 0.56 of the light within its nominal 0.26 NA acceptance cone.

**APPENDIX C**  
**SIDE-LIGHT CORRECTION FACTOR,  $\eta_s$ , FOR EDGE-EMITTER LEDs**

The measured total power from edge-emitter LEDs includes light from both the face and the sides of the LED, figure C-1.

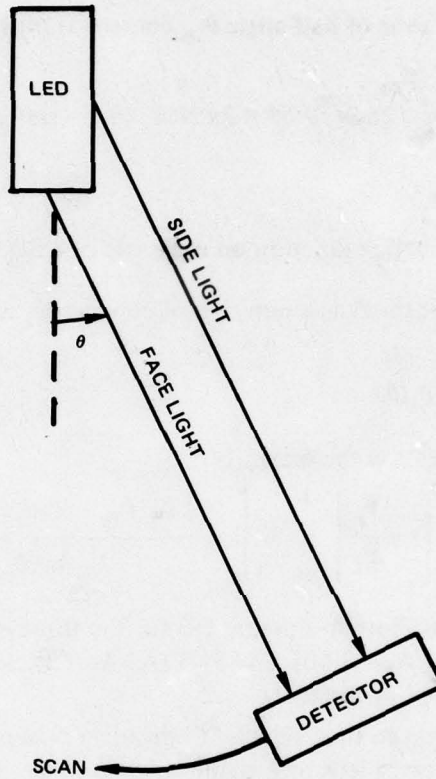


Figure C-1. Light emitted from the sides of the LED is not coupled into the fiber.

To compute the relative intensities of the light emitted by the face and the light emitted by the sides, (see figure C-2) assume that the power is uniformly emitted by each unit length of emitting junction along the face and sides of the LED edge-emitter and that it is lambertian. The light in the direction of the fiber from the face is then

$$P_f(\theta) = N A_f \int_0^{\theta_m} 2\pi \sin\theta \cos\theta \, d\theta = \pi N A_f \sin^2 \theta_m \quad (C-1)$$

where

$P_f(\theta)$  = power within a cone of half-angle  $\theta_m$  from the face

$N$  = radiance of LED

$A_f$  = area of emitting junction face

The power within the cone of half-angle  $\theta_m$  emitted from sides is

$$P_s(\theta) = 2N A_s \int_0^{\theta_m} 2\pi \sin^2\theta \, d\theta = 2\pi N A_s (\theta_m - \sin\theta_m \cos\theta_m) \quad (C-2)$$

where

$A_s$  = area of emitting junction on each side of LED

The "total power," measured as a function of cone angle, is then the sum of equations C-1 and C-2.

$$P(\theta) = P_f(\theta) + P_s(\theta) \quad (C-3)$$

and the side light correction factor,  $\eta_s$ , is

$$\eta_s = \frac{P_f}{P_f + P_s} = \left[ 1 + \frac{P_s}{P_f} \right]^{-1} = \left[ 1 + \frac{2 A_s (\theta_m - \sin\theta_m \cos\theta_m)}{A_f \sin^2\theta_m} \right]^{-1} \quad (C-4)$$

This equation is plotted in figure C-3 for the three edge-emitter LED groups: B-C ( $A_s/A_f = 1.4$ ), D-E ( $A_s/A_f = 3.60$ ), and F-H ( $A_s/A_f = 2$ ), where the letter designations refer to table 10 and figure 17 of the text.

A better solution to the "side-light" problem is to measure LED emitted power using a microradiometer: a lens of variable NA images the LED emitting area (excluding the sides) onto a variable aperture adjacent to the detector. This method yields the emitted power directly as a function of NA and core size and eliminates contributions from side light.

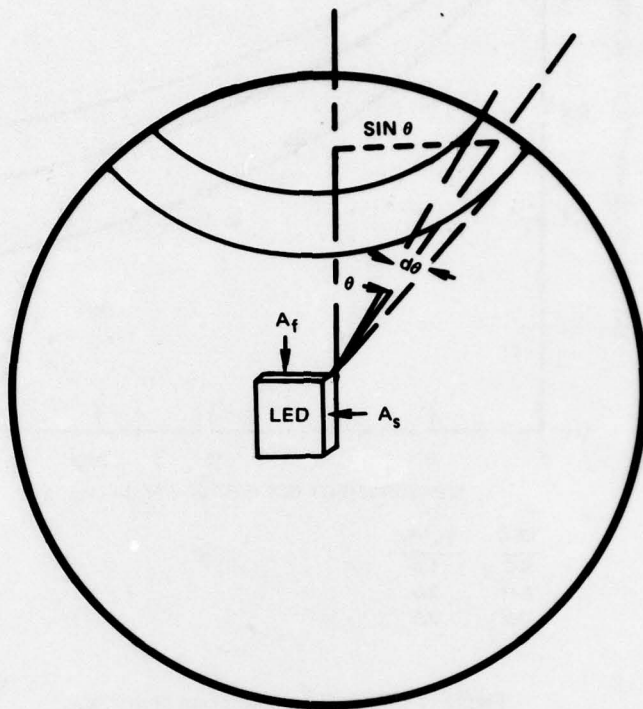


Figure C-2. Geometry for computing relative intensities of light emitted from face ( $A_f$ ) and sides ( $A_s$ ) of edge-emitter LEDs.

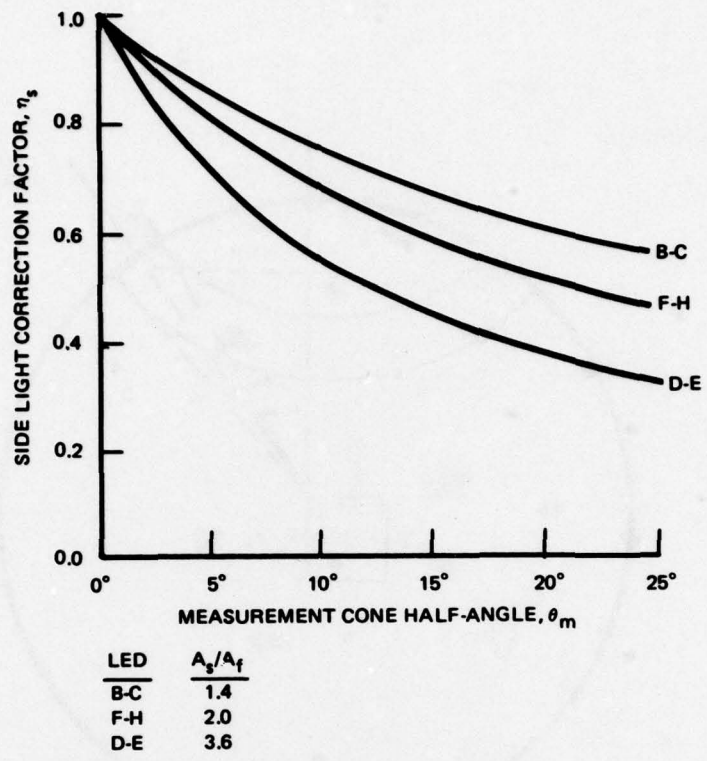


Figure C-3. Side-light correction factor,  $\eta_s$ .

## APPENDIX D RECEIVER SENSITIVITY

The required optical power for reliable detection is the function of the detector responsivity (the conversion of input optical power to output photocurrent) and receiver noise. For a  $10^{-8}$  BER, the equation relating these parameters is:<sup>D-1</sup>

$$\frac{i_S}{\langle i_N \rangle} = \frac{rP_D}{\langle i_N \rangle} = 11.22 \text{ (that is 21 dB)} \quad (\text{D-1})$$

where

$$\begin{aligned} i_S &= \text{peak detector signal current} \\ \langle i_N \rangle &= (i_n^2)^{1/2} = \text{rms noise current of receiver} \\ P_D &= \text{peak optical power at detector} \\ r &= \text{detector responsivity} \end{aligned}$$

The detector responsivity is a function of the wavelength of light detected. Two wavelengths are required in the duplex link: such as one in the 0.8 to 0.9  $\mu\text{m}$  region and one in the 1.0 to 1.3  $\mu\text{m}$  region. Silicon detectors are suitable for the first region; no suitable detectors are available presently for the second at wavelengths longer than approximately 1.06  $\mu\text{m}$ .

The receiver noise,  $\langle i_N \rangle$  consists of detector dark current noise and amplifier noise

$$\langle i_N \rangle = (i_D^2 + i_A^2)^{1/2} \quad (\text{D-2})$$

The dark current noise is<sup>D-2</sup>

$$i_D^2 = 2eI_D B \quad (\text{D-3})$$

where

$$\begin{aligned} e &= \text{charge on electron} \\ I_D &= \text{dark current} \\ B &= \text{equivalent noise bandwidth} \end{aligned}$$

The amplifier noise for an FET preamplifier is<sup>D-2</sup>

$$i_A^2 = 2eI_L B + \frac{4kTB}{R_f} + \frac{4}{3}\pi^2 C_i^2 B^3 e_n^2 \quad (\text{D-4})$$

where

$$I_L = \text{FET gate leakage current}$$

D-1. Yariv, A., Introduction to Optical Electronics, 2nd Ed, 1976, Holt, Rinehart, Winston, 292, 331.

D-2. Gaell, J. E., An Optical Repeater With High Impedance Input Amplifier, BSTJ, 53, No 4, 629 (April 1974).

$k$  = Boltzmann's constant  
 $T$  = absolute temperature  
 $R_f$  = feedback resistor  
 $C_i$  = total input capacitance of preamplifier  
 $e_n$  = FET channel noise voltage

A receiver constructed at NOSC was optimized for operation at  $0.85 \mu\text{m}$  at a 50 kb/s data rate. The relevant characteristics are summarized below:

$I_D = 100 \text{ pA}$  (dark current at 10 V reverse bias)  
 $I_L = 20 \text{ pA}$  (gate leakage current at  $25^\circ\text{C}$ )  
 $B = 30 \text{ kHz}$   
 $R_f = 125 \text{ M}\Omega$   
 $C = 13 \text{ pF}$   
 $e_n = 4 \times 10^{-9} \text{ V}/\sqrt{\text{Hz}}$

Substituting these values into eq D-3 and D-4 gives an equivalent input noise of

$$\langle i_N \rangle = 2.5 \text{ pA}$$

The measured value<sup>D-3</sup> was 3.9 pA.

The photodiode responsivity is approximately  $0.4 \text{ A/W}$  at  $0.85 \mu\text{m}$ , yielding a minimum required peak-to-peak optical power of  $100 \text{ pW}$  ( $-70 \text{ dBm}$ ). The measured optical power for  $10^{-8}$  BER was  $-65 \text{ dBm}$ .

The performance of the receiver at  $1.06 \mu\text{m}$  using an RCA type C30812 silicon detector (optimized for  $1.06 \mu\text{m}$  response) can be estimated using equations (11-14) with the following values:

$r = 0.5 \text{ A/W}$  at  $1.06 \mu\text{m}$   
 $I = 20 \text{ nA}$  at 10V reverse bias

The equivalent noise input current is  $14 \text{ pA}$  and the required pk-pk optical power is  $340 \text{ pW}$  ( $-64.7 \text{ dBm}$ ), or approximately 5 dB more than that of the  $0.85 \mu\text{m}$  detector.

---

D-3. NOSC TR 297, "Fiber Optic Sonobuoy Cable Development FY77," by R. A. Eastley and W. H. Putnam, 15 August 1978.